Models of the Hofstadter Type

Ch. Kreft * and R. Seiler
Fachbereich Mathematik, Technische Universität Berlin
10623 Berlin, Germany

May 11, 1996

Abstract

Spectra and eigenfunctions of discrete hamiltonians are computed using algebraic, analytic und nummerical tools. In particular we consider the Hofstadter and the Second Neighbor Square Lattice model, the Triangular Lattice model in an inhomogenous magnetic field, the Doubly-discrete Quantum Pendulum and the Honeycomb model. Qualitative properties of the spectra are related to symmetries.Semiclassical analysis in the algebraic setting for the Doubly-discrete Quantum Pendulum is shown to match nummerical results well. The connection to integrable models is mentioned.

PACS: 71.- 73.-

* Present adress: IVU-Gellschaft für Informatik, Verkehr und Umweltplanung mbH, 12161 Berlin, Bundesallee 88

1 Introduction

The subject of this article lies on the edge of physics, mathematics and computer science. It concerns the analysis of some quantum mechanical models for transport phenomena in two–dimensional solids.

Since many decades it is well–known that transport of electrons shows remarkable properties. Collective behaviour of particles leads often to situations where charge transport can be described best in terms of quasiparticles. They can have positive, negative or even non integer charge. Of particular interest are phenomena which are seen in two dimensional systems in the presence of large magnetic fields and at low temperature. It is there where integer or fractional quantum Hall conductance is observed.

Such phenomena can be modeled in part by Hamiltonians of the Hofstadter type. These operators have interesting mathematical properties. Their spectra are typically fractal and charge transport is integral.

There are several computational methods for dealing with Hamiltonians of the Hofstadter type. For the computation of spectra Chambers formula (see section V, theorem 1) is most useful [14]. Dynamics of wave functions can be visualized best in terms of Husimi functions (see section II and section III).

The elementary objects which underly the construction of all model Hamiltonians are the discrete magnetic translations [52]. We will give a systematic exposition of these operators in terms of Weyl operators in the following section. At this point let us just adopte a pragmatic point of view and discretize the well–known expressions for a charged particle in a constant magnetic field in the most straightforward way:

Let Ψ be a function on $\mathbb{Z}^2$ with values in $\mathbb{C}$ and $\chi = (\chi_1, \chi_2)$ a discrete and real valued vectorpotential such that

$$\operatorname{curl}\chi(n) := \partial_1\chi_2 - \partial_2\chi_1 = \Phi \ . \tag{1}$$

Discrete derivatives are defined by

$$\partial_j F(n) := F(n) - F(n - e_j), \qquad (j = 1, 2), \tag{2}$$

and magnetic translations [1] as follows:

$$T_1\Psi(n) = e^{i\,\chi_1(n)}\ \Psi(n_1 - 1, n_2) \tag{3}$$

$$T_2\Psi(n) = e^{i\,\chi_2(n)}\ \Psi(n_1, n_2 - 1) \ . \tag{4}$$

They are unitary on $\ell^2(\mathbb{Z}^2)$. Due to the phase in their definition they have an elementary holonomy

$$T_1^{-1}\ T_2^{-1}\ T_1\ T_2 = e^{i\,\Phi} \ . \tag{5}$$

$(1 - T_1)$ and $(1 - T_2)$ are discrete magnetic momentum operators and give rise to the magnetic discrete Laplacian

$$\triangle = \sum_{\ell=1}^{2}\ (1 - T_\ell)^*\ (1 - T_\ell) \ . \tag{6}$$

[1] The magnetic translations can be interpreted as connections on the trivial discrete vector bundle $\mathbb{Z}^2 \times \mathbb{C}$. Equation (1) defines χ in terms of Φ up to a discrete gradient $(\partial_1\varphi, \partial_2\varphi)$, where φ denotes a function on $\mathbb{Z}^2$ generating a discrete gauge transformation.

coinciding with the Hofstadter Hamiltonian up to a sign and an additive constant.

$$H_{Hof} \;=\; T_1 + T_2 + T_1^* + T_2^* \;. \tag{7}$$

The Hofstadter model has several physical interpretations. The most prominent one is as a tight-binding approximation for electrons bound to atomic sites in a two-dimensional crystal and in a strong external magnetic field. It is a model with two typical frequencies. The first corresponding to the area of the unit cell in the lattice, the second to the flux through a unit cell, which in our notation is Φ.

The history of the Hofstadter model goes back to the work of Peierls [41] on Bloch electrons in metals under the influence of a magnetic field. In the fifties and sixties progress was made by Azbel [1], Harper [24], Zak [52], Chambers [14] and Langbein [37]. They discovered the role of magnetic translations and began a systematic study of the square lattice model.

In 1976, Hofstadter [32] published the famous Hofstadter butterfly (Fig.3). He found that the figure of the spectral bands versus the magnetic flux exhibits a complicated yet beautiful fractal structure. A detailed study of the square lattice and other models began thereafter. We just mention work by Wilkinson [50] who related the fractal structure to a WKB analysis of tunneling between different lattice cells. This semi-classical approach was put in a rigorous form by Helffer and Sjöstrand [27, 29, 30, 31, 26] using pseudo-differential operator calculus. This work was recently simplified and completed by Buslaev and Fedotov [10, 11, 9, 12, 13] by means of a WKB-approach for difference equations. Since the Hofstadter model turns into Harper's equation by a Bloch-wave ansatz, the spectral analysis of the two models is the same. About the latter and its generalisation, the Discrete Mathieu model, detailed results are known. Let us mention just one, the theorem by Last and Wilkinson about the total length of the band spectrum S for the critical value $\lambda = 2$ (Harper's equation) and magnetic flux $\phi = 2\pi p/q$ [40, 38]:

$$\frac{2(\sqrt{5}+1)}{q} < S < \frac{8e}{q} \tag{8}$$

For more details we refer to the recent articles by Last, Jitomirskaya and Shubin [39, 34, 45]. In parallel, the algebraic study was put forward by Bellissard [3, 4, 5], who related the Hofstadter model to the work of A. Connes [18] on non-commutative geometry.

It was a big surprise at the beginning of the nineties when it turned out that the Quantum Discrete Sine-Gordon equation [22, 7] leads to the Hofstadter model [7]. Presently, Quantum groups and the Bethe Ansatz in the context of the Hofstadter model receive considerable attention [49], [21], [33].

Hamiltonians of the Hofstadter type like the Hofstadter Hamiltonian, the triangular, the hexagonal model or the Doubly-discrete Quantum Pendulum are the main objects of analysis in this article. They are all elements of a C^*–algebra generated by the magnetic translations, the so–called rotation algebra which is a particular case of a Weyl-Heisenberg algebra. Furthermore they can be understood as pseudodifferential operators on the circle. In this set-up the classical symbol of the Hofstadter Hamiltonian is

$$H_{Hof}\ (\xi, x) = \cos\xi + \cos x \;. \tag{9}$$

It is defined on phase space $S^1 \times S^1$ with the natural symplectic structure. For a list of the Hamiltonians discussed in this article and their symbols, we refer to Table 2.

Many of these Hamiltonians allow for a completely different interpretation: they are quantum integrals of a dynamical automorphism of the rotation algebra. Consider e.g. the Hamiltonian of the Doubly-discrete Quantum Pendulum for $k \in \mathbb{R} \setminus \{0\}$,

$$\begin{aligned} H_{QP} &= 2(T_1 + T_2 + T_1^* + T_2^*) + k(e^{-\frac{i\Phi}{2}}\, T_1\, T_2 + e^{\frac{i\Phi}{2}}\, T_2^*\, T_1^*) \\ &\quad + \frac{1}{k}(e^{-\frac{i\Phi}{2}}\, T_2\, T_1^* + e^{\frac{i\Phi}{2}}\, T_1\, T_2^*) \ . \end{aligned} \tag{10}$$

It is invariant under the automorphism generated by the map

$$\alpha :\ \langle T_1, T_2 \rangle \mapsto \langle T_2, T_3 = T_1^* (\frac{k + e^{\frac{i\Phi}{2}}\, T_2}{1 + k\, e^{\frac{i\Phi}{2}}\, T_2})^2 \rangle \ . \tag{11}$$

This automorphism appeared first in the doubly discrete integrable sine–gordon theory [7, 22, 23]. [2]

The article is structured as follows. In the next section we formulate elementary discrete quantum mechanics. The groundstate of the elementary Hofstadter hamiltonian is shown to be unique and invariant under discrete Fourier transformation. All this lays the basics for the "Kinematics of the Hofstadter Type Models" which is the subject of the third section where there is some overlap with a recent article by Faddeev [20] on the Discrete Heisenberg-Weyl Group and the Modular Group. The discrete analog of the Landau momentum and the Landau velocity is introduced and combined to form generators of the quantum group SL_q. In the fourth section we discribe the models and present nummerical results. Symmetries are used to understand some qualitative properties of the spectra. The Husimi functions of the Doubly-discrete Quantum Pendulum are shown to be localized at the classical orbits. In the last section we discuss Chambers relation for the Doubly-discrete Quantum Pendulum and comment on semiclassical methods for the computation of spectra. The semiclassical results are shown to approximate the nummerical results well. For details on most of the material presented here we refer to [36].

Quantum group structures appear naturally in the context of the models of the Hofstadter type. It is hoped that this will eventually lead to a better understanding of the complicated and interesting nested structure of their spectra. This has, however, not yet materialized although we have worked in this direction for several years.

---

[2] In the continuum case the automorphism is generated by equation (12) below. It is a special case of the hyperbolic equation

$$(\partial_t^2 - \partial_x^2)\ \phi(b, x) + g \sin \phi(b, x) = 0 \ . \tag{12}$$

For space independent solutions $\phi(t)$ one gets the pendulum equation

$$\partial_t^2 \phi(t) + g \sin \phi(t) = o \ . \tag{13}$$

.

2 Elementary Discrete Quantum Mechanics

The irreducible state space for a discrete quantum system with one degree of freedom and rational Planck constant $\not{\Phi} = \frac{p}{q}$, where p and q are relatively prime, is the complex vector space $\mathbb{C}^q$. The canonical position and momentum operators are

$$t_1 = \begin{pmatrix} 0 & 0 & \dots & \dots & 0 & 1 \\ 1 & 0 & & & 0 & 0 \\ \vdots & \ddots & \ddots & & & \\ \vdots & & \ddots & \ddots & & \\ \vdots & & & \ddots & 0 & 0 \\ 0 & \dots & \dots & \dots & 1 & 0 \end{pmatrix} \tag{14}$$

and

$$t_2 = diag\ (e^{i\Phi}, e^{2i\Phi}, \dots, e^{iq\Phi}), \ \ \Phi = 2\pi \not{\Phi}\ . \tag{15}$$

The operators t_1 and t_2 have simple and remarkable properties listed below.

1. t_1 and t_2 satisfy the same commutation relations (5) as the magnetic translations T_1 and T_2 defined in section 1 formula (3).
2. They are, however, idempotent,
$$t_1^q = t_2^q = 1\ . \tag{16}$$
3. t_1 can be understood as a shift on the q–periodic doubly infinite sequences (which is naturally identified with $\mathbb{C}^q$).
4. t_1 and t_2 are related by discrete Fourier transformation
$$\begin{aligned} \mathcal{F} : \mathbb{C}^q &\to \mathbb{C}^q, \\ f(n) &\mapsto \widehat{f}(n) = \frac{1}{\sqrt{q}} \sum_m e^{inm\Phi}\ f(m), \end{aligned} \tag{17}$$
$$t_2 = \mathcal{F} t_1\ \mathcal{F}^{-1}\ . \tag{18}$$
Note that $\mathcal{F}$ is unitary, $\mathcal{F}^{-1} = \mathcal{F}^*$ and $\mathcal{F}^4 = 1$. Thus
$$\sigma(\mathcal{F}) \subset \{1, -1, i, -i\}\ . \tag{19}$$
5. t_1 and t_2 have the same invariants. Particularly for $q > 1$, one gets the equations
$$\begin{aligned} \det t_1 &= \det t_2 &= 1 \\ \mathrm{trace}\, t_1 &= \mathrm{trace}\, t_2 &= 0\ . \end{aligned} \tag{20}$$

The elementary Hofstadter Hamiltonian is the simplest non trivial selfadjoint operator made out of t_1 and t_2

$$h = t_1 + t_2 + t_1^* + t_2^* \ . \tag{21}$$

It is invariant under Fourier transformation. h is the elementary constituent of the Hofstadter amiltonian (see theorem 3 section 3 and remark 1 there after). Furthermore h (or rather, $4 - h$) is the discrete analog of the harmonic oscillator. Unfortunately, its ground state is not expressable in simple terms. Nevertheless, a partial characterization can be given as the following theorem shows:

<u>Theorem 1:</u>

i) $4 - h$ has a non-degenerate ground state, ω . There is a strictly positive choice for ω.

ii) ω is invariant under Fourier transformation.

<u>Proof:</u>

i) The first statement follows from the Perron–Frobenius theorem [44]. Consider the Hamiltonian $h + 3$. It has non-negative entries only. Furthermore, for each entry of the matrices the following inequality holds:

$$((h+3)^q)_{i,j} \geq ((t_1 + t_1^* + 1)^q)_{i,j}. \tag{22}$$

Next we replace t_1 by the nilpotent matrix D

$$D = \begin{pmatrix} 0 & 0 & \dots & \dots & 0 & 0 \\ 1 & 0 & & & 0 & 0 \\ \vdots & \ddots & \ddots & & & \\ \vdots & & \ddots & \ddots & & \\ \vdots & & & \ddots & 0 & 0 \\ 0 & \dots & \dots & \dots & 1 & 0 \end{pmatrix} \tag{23}$$

and obtain the inequality

$$(t_1 + t_1^* + 1)^q \geq (D + D^* + 1)^q \geq \sum_{\ell=1}^{q} (d^\ell + d^{*\ell}) + 1. \tag{24}$$

Hence each entry of the matrix $(h+3)^q$ is larger than one; therefore, $h+3$ is ergodic.

ii) Since $\mathcal{F}$ commutes with h, there is a choice of ω which is an eigenvector of $\mathcal{F}$ too:

$$\mathcal{F}\omega = \lambda\omega \tag{25}$$

for some $\lambda \in \{+1, -1, -i, +i\}$.

Consider now the last component in the equation above,

$$\frac{1}{\sqrt{q}} \sum e^{iq\ell\Phi} \; \omega(\ell) = \frac{1}{\sqrt{q}} \sum \omega(\ell) = \lambda\omega(q) \; . \tag{26}$$

Since $\omega(i), \; i \in \{1, \dots, q\}$, is strictly positive this is consistent with $\lambda = 1$ only.

So it is well motivated to call the ground state ω of h a discrete version of the gauss–function. This is supported by numerical computations (see Fig.1).

Discrete quantum mechanics can also be formulated in terms of functions on discrete phase space $\mathbb{C}^q \times \mathbb{C}^q$. The transition from one formulation to the other is given by a discrete Bargmann transformation. This formulation is useful – as in the continuous case – for making contact with the corresponding classical theory.

Discrete position and momentum give rise to the Weyl operators $\mathrm{w}(m), \; m \in \mathbb{Z}^2$, defined by

$$\begin{aligned} \mathrm{w}(1,0) &= t_1 \qquad\qquad (27)\\ \mathrm{w}(0,1) &= t_2 \\ \mathrm{w}(m+n) &= \exp\,[-\frac{i}{2}\;\Phi\,\sigma(m,n)]\;\mathrm{w}(m)\;\;\mathrm{w}(n)\;, \qquad (m,n \in \mathbb{Z}^2)\;. \end{aligned}$$

$\sigma(m,n)$ denotes the standard discrete sympletic form

$$\sigma(m,n) := m_1\; n_2 - m_2\; n_1 . \tag{28}$$

Note that the discrete Weyl operator w is doubly q–periodic

$$\mathrm{w}(m+qn) = \mathrm{w}(m) \;, \qquad (m,n \in \mathbb{Z}^2) \;. \tag{29}$$

Fourier transformation acts on w like a rotation by $\frac{\pi}{2}$,

$$\mathcal{F}\mathrm{w}(m)\;\mathcal{F}^{-1} = \mathrm{w}(Jm) \;, \qquad (m = (m_1, m_2) \in \mathbb{C}^q \times \mathbb{C}^q) \;. \tag{30}$$

where J denotes the discrete complex structure $Jn = (-n_2, n_1), n \in \mathbb{Z}^2$.

In terms of the discrete Weyl operator w and the ground state ω of h, the discrete Bargmann transformation is defined by

$$
\begin{aligned}
B \,:\, \mathbb{C}^q &\;\to\; \mathbb{C}^q \times \mathbb{C}^q\,, \\
\psi &\;\mapsto\; B_\psi(m) := (\omega, \mathrm{w}(Jm)\psi)\ .
\end{aligned}
\tag{31}
$$

The action of all relevant operators on the state space $\mathbb{C}^q$ can now easily be transformed to the Bargmann representation.

In order to interpret wave functions in classical terms it is useful to look at the Husimi functions. They are usually defined in terms of Bargmann functions

$$
H_\psi(m) = |B_\psi(m)|^2\ . \tag{32}
$$

Notice, however, that they can also by given in terms of a trace over projectors in the original state space $\mathbb{C}^q$,

$$
H_\psi(m) = \mathrm{trace}\,[p_\psi\, \mathrm{w}(m)\ p_\omega w^{-1}(m)]\ . \tag{33}
$$

where p_ψ and p_ω denote the projectors onto ψ and ω, respectively.

3 Kinematics of Hofstadter Type Models

Kinematics of the Landau, the Hofstadter model, and their descendents are very close to each other. It is, therefore, natural to develop them in parallel. The basic object in the background of what follows is the Heisenberg group in $2+1$ one dimensions.It gives rise to the following family of unitary Weyl operators on $L^2(\mathbb{C})$,

$$W_\Phi(x)\ F(y) = \exp\ [\frac{i}{2}\ \Phi\sigma(x,y)]\ F(y-x)\ . \tag{34}$$

σ denotes the natural symplectic quadratic form on $\mathbb{C}$, $\sigma(x,y) = Im\ \overline{x}y = x_1y_2 - x_2y_1$, ($x = x_1 + i\,x_2 \in \mathbb{C}$), and Φ is a real parameter which is interpreted to be the magnetic flux through a surface of unit area.

The Weyl operators W_Φ satisfy the composition law

$$W_\Phi(x)\ W_\Phi(y) \quad = \quad \exp\ [\frac{i}{2}\Phi\sigma(x,y)]\ W_\Phi(x+y)\ , \tag{35}$$

which gives rise to the canonical commutation relation

$$W_\Phi(x)\ W_\Phi(y) = \exp\ [i\Phi\sigma(x,y)]\ W_\Phi(y)\ W_\Phi(x)\ . \tag{36}$$

Equations (34) and (36) have nice and simple geometric interpretations [3].

The operators $W_{-\Phi}$ commute with the W_Φ's. In fact, it can be proved [45] that the commutand of the von Neumann algebra generated by the W_Φ's is equal to the von Neumann algebra generated by the $W_{-\Phi}$'s and vice versa,

$$\{W_\Phi(x) \mid x \in \mathbb{C}\}' = \{W_{-\Phi}(x) \mid x \in \mathbb{C}\}''\ . \tag{37}$$

The operators W_Φ and $W_{-\Phi}$ form two commuting two-parametric, strongly continuous unitary groups and are, therefore, generated by self-adjoint operators, v and k, as follows.

[3] $W_\Phi(x)$ is the intergrated connection $\nabla = d + iA,\ dA = \Phi\ dx^1 \wedge dx^2$ on $\mathbb{C}\times\mathbb{C}$. Furthermore W_Φ is a projective representation of the abelian group $\mathbb{C}$, and at the same time a non–commutative deformation of the characters of $\mathbb{R}^2$.

$$
\begin{aligned}
W_\Phi(x) &= \exp\, ix\cdot v \qquad x\cdot v = x_1v_1 + x_2v_2 \\
v_1 &= i\partial_1 - \frac{\Phi}{2}\, y_2 \\
v_2 &= i\partial_2 + \frac{\Phi}{2}\, y_1 \\
W_{-\Phi}(x) &= \exp\ ix\cdot k\ , \qquad x\cdot k = x_1k_1 + x_2k_2 \\
k_1 &= i\partial_1 + \frac{\Phi}{2}\, y_2 \\
k_2 &= i\partial_2 - \frac{\Phi}{2}\, y_1\ .
\end{aligned} \tag{38}
$$

The commutation relations (36) imply

$$
\begin{aligned}
[v_1, v_2] &= i\Phi \\
[k_1, k_2] &= -i\Phi \\
[k_n, v_n] &= 0\ , \qquad m, n \in \{1, 2\}\ .
\end{aligned} \tag{39}
$$

In physical terms, v is the velocity and k the momentum operator. From k, one derives the operator $c = \frac{1}{\Phi^2}\ (k \wedge \Phi)$ which is the operator of the Landau center [4]. It has the commutation relations

$$
[c_1, c_2] = -\frac{i}{\Phi}\ . \tag{40}
$$

The magnetic flux Φ plays a role much like Planck's constant in quantum mechanics. This analogy leads naturally to quantization of arbitrary functions on phase space. Let F be an element of the Schwartz test function space and $\widehat{F}$ its Fourier transformation. The corresponding quantization is naturally [5] defined by

$$
W_\Phi(F) = (\frac{1}{2\pi})\ \int dx\ \widehat{F}(x)\ W_\Phi(x)\ . \tag{41}
$$

These operators generate a C^*–algebra (norm closure) or a von Neumann algebra (weak closure) respectively. According to the von Neumann uniqueness theorem the von Neumann algebra has irreducible constituents which are all equivalent to the standard Schrödinger representation.

[4] The expectation value of the position operator circles around the expectation value of c according to the dynamics of the Landau Hamiltonian. Furthermore c is an integral of motion.

[5] The definition below produces a non–commutative Φ–deformation of the algebra of functions on phase space $\mathbb{C}$.

Kinematics of the models of the Hofstadter type are a discrete version of the one for the Landau model described above. Consider the discrete phase space $\mathbb{Z}^2$ and the standard discrete symplectic structure σas defined before (28).

The corresponding Weyl operators on $\ell^2(\mathbb{Z}^2)$ are defined by

$$W_\Phi(m)\ F(n) = \exp\ [\frac{i}{2}\ \Phi\sigma(m,n)]\ F(n-m)\ . \tag{42}$$

They satisfy again the Weyl relations,

$$W_\Phi(m)\ W_\Phi(n) = \exp\ [\frac{i}{2}\ \Phi\sigma(m,n)]\ W_\Phi(m+n)\ , \tag{43}$$

$$\tag{44}$$

$$W_\Phi(m)\ W_\Phi(n) = \exp\ [i\Phi\sigma(m,n)]\ W_\Phi(n)\ W_\Phi(m) \tag{45}$$

Equations (42) and (43) again have simple geometric interpretations in terms of connections on a discrete complex line bundle over $\mathbb{Z}^2$.

The discrete Weyl operators $W_{-\Phi}$ commute with the $W_\Phi\,'s$ and they generate their respective commutant.

$$\{W_\Phi(n)\mid n\in\mathbb{Z}^2\}' = \{W_{-\Phi}(m)\mid m\in\mathbb{Z}^2\}''\ . \tag{46}$$

The operators W_Φ and $W_{-\Phi}$ form 2–parametric, discrete unitary groups. They are generated by the elementary pairs of unitary operators

$$\begin{array}{rcl} T_1^{(v)} & := & W_\Phi(1,0) \\ T_2^{(v)} & := & W_\Phi(0,1) \end{array} \tag{47}$$

and

$$\begin{array}{rcl} T_1^{(k)} & := & W_{-\Phi}(1,0) \\ T_2^{(k)} & := & W_{-\Phi}(0,1) \end{array} \tag{48}$$

respectively and satisfy the relations

$$\begin{array}{rcl} T_1^{(v)}\ T_2^{(v)} & := & e^{i\Phi}\ T_2^{(v)}\ T_1^{(v)} \\ T_1^{(k)}\ T_2^{(k)} & = & e^{-i\Phi}\ T_2^{(k)}\ T_1^{(k)}\ . \end{array} \tag{49}$$

In physical terms $T^{(v)}$ is the discrete velocity and $T^{(k)}$ the discrete momenum operator.

Each pair $(T_1^{(v)}, T_2^{(v)}), (T_1^{(k)}, T_2^{(k)})$ generates a rotation algebra. Together they have a natural structure as a quantum group SL_q, $q = e^{i\Phi}$ [6].

In the following we will mostly use the first pair, $T_1^{(v)}$, $T_2^{(v)}$. To simplify notation we drop the upper index from now on and simply write $T_1 := T_1^{(v)}$, $T_2 := T_2^{(v)}$. Furthermore we replace $W_\Phi(n)$ by $W(n)$.

Quantization of phase space functions, $f \in C^\infty(T^2)$, where T^2 denotes the two-torus, given by

$$W(f) = \sum \hat{f}(m)\ W(m)\ , \qquad (f(x) = \sum \hat{f}(m)\ e^{imx}) \tag{54}$$

leads to the C^*–algebra $\mathcal{C}_\Phi$ and the von Neumann algebra $\mathcal{N}_\Phi$ by norm and weak closures respectively. To fix the notation, let us call $\mathcal{C}_\Phi$ the rotation algebra and $\mathcal{N}_\Phi$ the Weyl-Heisenberg algebra. [7]. f is the classical symbol of the operator $W(f)$.

There is a natural trace on the C^*–algebra generated by the Weyl operators $W(f)$

$$\text{trace}\ \ W(f) = \hat{f}(0)\ . \tag{55}$$

The GNS construction with respect to this trace leads back to the representation (42) we started from .

[6] Each pair forms a degenerate representation of a quantum group SL_q with the L–operators

$$\begin{aligned} L^{(v)} &= \begin{pmatrix} T_1^{(v)} & T_2^{(v)} \\ 0 & T_1^{(v)*} \end{pmatrix} \\ L^{(k)} &= \begin{pmatrix} T_2^{(k)} & 0 \\ T_1^{(k)} & T_2^{(k)*} \end{pmatrix} . \end{aligned} \tag{50}$$

Since $L^{(v)}$ and $L^{(k)}$ satisfy the Yang–Baxter equation

$$R_{12} L_1^{(\sigma)} L_2^{(\sigma)} = L_2^{(\sigma)} L_2^{(\sigma)} R_{12}\ , \qquad (\sigma \in \{v, k\}), \tag{51}$$

the same is true for their tensor product

$$L^{(v)} \otimes L^{(k)} = \begin{pmatrix} T_1^{(v)} T_2^{(k)} + T_2^{(v)} T_1^{(k)} & T_2^{(v)} T_2^{(k)*} \\ T_1^{(v)*} T_1^{(k)} & T_1^{(v)*} T_2^{(k)*} \end{pmatrix} . \tag{52}$$

The R–matrix is the canonical one

$$R = \begin{pmatrix} q & 0 & 0 & 0 \\ 0 & 1 & q - \frac{1}{q} & 0 \\ 0 & 0 & 1 & 0 \\ 0 & 0 & 0 & q \end{pmatrix} . \tag{53}$$

By construction the q–determinant is one.

[7] The above definition produces a non–commutative Φ–deformation of the algebra of functions on the torus. In the terminology of Connes this is the quantized torus.

It is well–known that all irreducible representations of the Weyl-Heisenberg algebra $\mathcal{N}_\Phi$ for rational $\not{\Phi} = \dfrac{\Phi}{2\pi}$ can explicity be written in terms of finite dimensional matrices.

Theorem 2:

Let the magnetic flux be rational, $\Phi = 2\pi\,\dfrac{p}{q}$ and p, q relatively prime. Then all irreducible representations of $\mathcal{N}_\Phi$ are labelled by an element of the torus $S^1 \times S^1$. The representation π_θ is, up to unitary conjungation, defined by

$$\begin{array}{rcl} \pi_\theta(T_1) & = & e^{i\theta_1}\; t_1, \\ \pi_\theta(T_2) & = & e^{i\theta_2}\; t_2\;, \end{array} \tag{56}$$

where t_1 and t_2 are the discrete momentum and the discrete position operators introduced in Chapter 2, formula (14) and (15).

The irreducable representations π_θ have several interesting properties which are in part just translations from the corresponding properties of t_1 and t_2 :

1. Representations $\pi_\theta,\ \theta \in S^1 \times S^1$ are not injective since T_1^q and $e^{iq\theta_1}\,.\mathbb{1}$ have the same image under the map π_θ.
2. Two representations π_θ and $\pi_{\theta'}$ for $\theta \neq \theta'$ and $(\theta, \theta') \in [0, \frac{2\pi}{q}) \times [0, \frac{2\pi}{q})$ are inequivalent because the spectra of $\pi_\theta(T_\ell)$ and $\pi_{\theta'}(T_\ell),\ \ell = 1, 2$, are different.
3. If however $\theta' = \theta + \frac{2\pi}{q}\ m$ for $m \in \mathbb{Z}^2$, the two representations $\pi_{\theta'}$ and π_θ are equivalent. The unitary intertwining between $\pi_{\theta'}$ and π_θ is constructed as follows: From the commutation relations of the Weyl operators we conclude that for every $n \in \mathbb{Z}^2$ and $A \in \mathcal{N}_\Phi$

$$\pi_{\theta+\Phi n}(A) = W(J\,n)\ \pi_\theta(A)\ W^{-1}(J\,n)\ . \tag{57}$$

Since furthermore the Diophantine equation for r, s in $\mathbb{Z}$

$$pr + qs = 1 \tag{58}$$

has a solution – due to the Euclidean algorithm – we find, for every $m \in \mathbb{Z}^2$, an element $n \in \mathbb{Z}^2$ such that

$$\not{\Phi} n = \frac{m}{q} \quad \text{modulo}\, 1. \tag{59}$$

For rational $\not{\Phi}$, the von Neumann algebra $\mathcal{N}_\Phi$ is of Type–I_q, where $\not{\Phi} = \dfrac{p}{q}$, p and q relatively prime. This situation changes if $\not{\Phi} \notin Q$. In this case the center $\mathcal{N}_\Phi \cap \mathcal{N}_\Phi{}' = \mathbb{C}\mathbb{1}$, hence $\mathcal{N}_\Phi$ is a factor. In fact $\mathcal{N}_\Phi$ is a II_1–Factor because the trace defined by (55) is weakly continuous and strictly positive [45].

The representation of the Weyl algebra $\mathcal{N}_\Phi$ for rational $\not{\Phi}$ is reducible. In fact each irreducible representation appears exactly once. This is the content of the following theorem which we cite with no proof:

<u>Theorem 3:</u> For rational $\not{\Phi} = \frac{p}{q}$, p and q relatively prime , there exists a unitary transformation

$$U \; : \; \ell^2(\mathbb{Z}^2) \; \rightarrow \; \frac{1}{|\mathcal{B}|} \int_{\mathcal{B}}^{\oplus} d^2\theta \; \mathbb{C}^q \otimes \mathbb{C}^q \tag{60}$$

such that

$$\begin{aligned} T_\alpha^{(v)} \;&\cong\; \frac{1}{|\mathcal{B}|} \int_{\mathcal{B}}^{\oplus} d^2\theta \, \pi_\theta(T_\alpha) \otimes \mathbb{1} \\ T_\alpha^{(k)} \;&\cong\; \frac{1}{|\mathcal{B}|} \int_{\mathcal{B}}^{\oplus} d^2\theta \, \mathbb{1} \otimes \pi_\theta(T_{\alpha+1}) \; , \qquad (\alpha \in \mathbb{Z}_2) \; . \end{aligned} \tag{61}$$

Here ,$\cong$ denotes equality up to conjugation by U and $\mathcal{B}$ denotes the magnetic Brillouin torus,

$$\mathcal{B} = \mathbb{R}(mod\frac{2\pi}{q}) \times \mathbb{R}(mod\frac{2\pi}{q}). \tag{62}$$

Theorem 3 has several useful consequences:

1. The spectral analysis of an element A of $\mathcal{N}_\Phi$ can be reduced to the analysis of its restriction to each individual fiber since

$$A \;\cong\; \frac{1}{|\mathcal{B}|} \int_{\mathcal{B}}^{\oplus} d^2\theta A(\theta) \otimes \mathbb{1} \; , \tag{63}$$

$$\sigma(A) \;=\; \bigcup_{\theta\in\mathcal{B}} \sigma(\pi_\theta(A)) \; . \tag{64}$$

   This means, in particular, that the spectral analysis of a Hamiltonian of the Hofstadter type is reduced to a matrix problem, e.g.

$$\sigma(H_{Hof}) = \bigcup_{\theta \in \mathcal{B}} \sigma(H_{Hof}(\theta)) \tag{65}$$

$$H_{Hof}(\theta) = e^{i\theta_1}\ t_1 + e^{i\theta_2}\ t_2 + e^{-i\theta_1}\ {t_1}^* + e^{-i\theta_2}\ {t_2}^* \tag{66}$$

where we used the notation $H_{Hof}(\theta) = \pi_\theta(H_{Hof})$.

2. The commutand of $\mathcal{N}_\Phi$ is given by the formula

$$\mathcal{N}_\Phi' = \mathrm{End}\,(L^2(\mathcal{B})) \otimes \mathbb{1} \otimes \mathrm{End}\,(\mathbb{C}^q)\ , \tag{67}$$

where $\mathrm{End}\,(L^2(\mathcal{B}))$ and $\mathrm{End}\,(\mathbb{C}^q)$ denote the spaces of bounded linear operators on $L^2(\mathcal{B})$ and $\mathbb{C}^q$ respectively. [8].

As a last subject in this section we mention a useful property of the Husimi functions. Let $\Psi(\theta)$ be an eigenvector of $H(\theta) = \pi_\theta(H), (\theta \in \mathcal{B})$, where H denotes a Hamiltonian which by assumption is an element of the von Neumann algebra $\mathcal{N}_\Phi$. Due to equation (57) one gets for the Husimi function

$$H_{\Psi(\theta)}(n) := |(w, W(J\,n)\Psi(\theta))|^2 \tag{68}$$

the equation

$$H_{\Psi(\theta)}(n) = H_{\Psi(\theta+\Phi n)}(0) \qquad , (n \in \mathbb{Z}^2, \theta \in \mathbb{R}^2)\ . \tag{69}$$

It defines a natural interpolation $H_{\Psi(\theta)}(x)\,, x \in \mathbb{R}$, between the discrete values of $H_{\Psi(\theta)}(n)$:

$$H_{\Psi(\theta)}(n) = H_{\Psi(\theta+\Phi n)}(0) \qquad , (n \in \mathbb{Z}^2, \theta \in \mathbb{R}^2)\ . \tag{70}$$

In particular, one gets the formula

$$H_{\Psi(0)}(\theta) = H_{\Psi(\Phi\theta)}(0) \qquad , \left(\theta \in \mathbb{R}^2\right)\ . \tag{71}$$

[8]We used the natural identification of $\frac{1}{|\mathcal{B}|} \int_{\mathcal{B}}^{\oplus} d^2\theta\ \mathbb{C}^q \otimes \mathbb{C}^q$ with $L^2(\mathcal{B}) \otimes \mathbb{C}^q \otimes \mathbb{C}^q$.

4 The Models

There are many automorphisms of the discrete Weyl–Heisenberg algebra, some are linear others are nonlinear - some are inner others not. We have not studied them systematically. This would be an interesting mathematical problem in itself. However we will give a list of examples. Many of them will show up later as symmetries of model Hamiltonians.

The simplest class of automorphisms are the linear ones. They may be called discrete Bogoliubov–Valatin transformations:

Proposition: Let M be a 2x2 matrix with integer entries and nonvanishing determinant. Then the map

$$\alpha_M : W(m) \to W(Mm) \qquad , \left(m \in \mathbb{Z}^2\right) . \tag{72}$$

generates an algebra homomorphism from $\mathcal{N}_\Phi$ onto $\mathcal{N}_{\det M.\Phi}$.

The statement follows directly from the commutation relations (45). The discrete Fourier transformation implements a special case of a discrete linear automorphism

$$W(m) = \mathcal{F}\, W(Jm)\mathcal{F}^{-1} \tag{73}$$

where J denotes the discret complex structure introduced before. Others are summarized in Table 1.

Nonlinear automorphisms are typically generated by an arbitrary function f which maps the unit circle into itself. In terms of magnetic translations they are defined by the shift

$$\begin{aligned} \alpha_f \quad : \quad & (T_1, T_2) \to (T_2, T_3) \\ & T_1 T_3 = f\,(T_2) \end{aligned} \tag{74}$$

where T_3 is defined by (74). It is easy to check that α_f is an algebra automorphism as long as all quantities encountered on the way of verification are well defined. (This requires some regularity for f). A particularly nice example is the one arising from the Doubly-discrete Quantum Pendulum [7] where

$$f_{QP}(z) = \frac{k + e^{i\phi/2}\; z}{i + k e^{i\phi/2}\; z}, \tag{75}$$

k is a real parameter defining the model; it is related to discrete curvature.

The algebra automorphism generated by f_{QP} is a symmetry of the Hamiltonian

$$\begin{aligned} H_{QP} &:= 2(W(1,0)+W(1,0)^*+W(0,1)+W(0,1)^*) \\ &+ k(W(1,1)+W(1,1)^*)+\frac{1}{k}(W(1,-1)+W(1,-1)^*), \end{aligned} \tag{76}$$

$$\alpha_{f_{QP}}(H_{QP}) = H_{QP}.$$

Put differently, H_{QP} is a quantum integral of the dynamics generated by $\alpha_{f_{QP}}$.

In the remaining part of this section we introduce several models of the Hofstadter type and mention their symmetries, from which one can deduce then some qualitative properties of their spectrum and eigenfunctions. Furthermore we show the results of numerical computations of spectra and eigenfunctions. In Table 2 the Hamiltonians of all these models are listed, together with their classical symbols.

All numerical computations of the spectra are based on Chamber's relation (see Section 5). This implies, in particular, that symmetries of classical symbols are reflected in spectral properties (see formula (108) in Section 5).

4.1 The Discrete Mathieu Model

The discrete Mathieu Hamiltonian describes an anisotropic variant of the Hofstadter model. It contains a real parameter μ which may be interpreted as the relative strength between the hopping interactions in the two lattice directions. The Hamiltonian is given by

$$H(\mu) = T_1 + \mu\, T_2 + T_1^* + \mu\, T_2^*. \tag{77}$$

For $\mu = 1$, we recover the Hofstadter Hamiltonian and, for $\mu = 0$, the one–dimensional discrete Laplacian which can be diagonalized explicitly. Hence μ interpolates between these limiting cases; therefore the discrete Mathieu model is a tool to derive properties of the Hofstadter model; e.g. in reference [46], the Chern number has been computed in this way. Other properties discussed by that method are the gap labelling[16], the total gap length and the spectrum for irrational flux (for recent results see Y. Last [38]).

In Table 3 the symmetries including the automorphism which gives rise to the Aubry duality are put together. [9] In the last column of the table, their consequence for the spectrum is shown. These symmetries can also be read off from the contour levels of the classical symbol (Fig.2). The spectra of the Hofstadter and the discrete Mathieu model are shown in Figure 3 and 4, respectively. In Figure 5, the Husimi function $H_{\Psi(0)}(n)$ for eigenstates of the Hofstadter model are shown. Small values are dark and large values white. The interpolation between the discrete values of n here and in the sequel are done using Equation (71) of Section 3.

4.2 The Second Neighbour Square Lattice Model

The model was discussed by Wilkinson already in 1984, [50]. Its Hamiltonian is given by the formula

[9] Notice that in our formulation the Aubry duality transformation is simply the linear automorphism generated by a rotation about the angle $\pi/2$.It is implemented by discrete Fourier transformation.

$$H_{SN}(\varepsilon) = T_1 + T_2 + \varepsilon\left(T_1^2 + T_2^2\right) + \text{ h.c.} \tag{78}$$

where ε denotes the relative strength of the coupling to the second neighbour in the lattice. Some qualitative properties of the spectrum (Fig. 6) follow already from the symmetries of the classical symbol (Tab.4). Wilkinson's computation of the spectrum showed a splitting of the lowest subband into a braid type structure (Fig 6, focus on the point flux = 0 and energy -2.4). This has been investigated in [2], and it was shown, that the braid structure can be understood as a phase space tunneling between the four bottom wells in the Brillouin torus (Fig.7).

4.3 The Triangular Lattice Model

The triangular model was introduced by Claro and Wannier [17] and describes a hexagonal cristal. They computed the spectrum nummerically and found a nesting structure similar to the one for the Hofstadter model was found. A semiclassical analysis was presented in [51]. In [6] the model was generalized to different fluxes in the two classes of triangles (Fig. 8). Its Hamiltonian is

$$H_{TR}(\eta) = T_1 + T_2 + e^{-i\eta}\, T_1\, T_2 + \text{ h.c.} \tag{79}$$

.

It is remarkable that also in this case the spectrum can be computed inspite of the spatial inhomogenity of the flux (Fig.9). This is possible because Chamber's relation still holds (Section 5). Numerical computations are in excellent agreement with semiclassical analysis [6]. Several qualitative aspects of the spectrum can already be understood by a simple consideration of symmetries (see Table 5).

4.4 The Honeycomb Lattice Model

This model has been introduced by Rammal [43] and is defined in terms of the Hamiltonian

$$H_{HC} = \begin{pmatrix} 0 & T_1 + T_2 + W(1,1) \\ T_1^* + T_2^* + W(1,1)^* & 0 \end{pmatrix} \tag{80}$$

He computed the spectrum numerically. The Hamiltonian linkes sites of a bibpartite lattice (Fig.10). This implies that the square of the Hamiltonian is just two independent triangular lattice models with, as it turns out, flux $\eta = 0$. Hence the computation can be reduced to the previous case (Fig.11) [6].

4.5 The Doubly-discrete Quantum Pendulum

Recently Bobenko, Kutz and Pinkall have introduced a family of Hamiltonians which arises in the analysis of the Doubly–discrete sine–Gordon equation [7],

$$\begin{aligned} H_{QP}(\varepsilon, k) &= \varepsilon\,(T_1 + T_2) + k\; W(1,1) + \\ &+ \frac{1}{k}\; W(1,-1) + \text{ h.c.} \end{aligned} \tag{81}$$

where ε and k are real parameters. For $\varepsilon = 2$, the Hamiltonian represents a quantum integral with respect to the automorphism defined by the Doubly–discrete sine–Gordon equation in zero spatial dimension (see Section 1, Eq. (11)). k is related to curvature.

The Hamiltonian H_{QP} in (81) belongs to the class of the next nearest neighbour Hamiltonians introduced by Hatsugai and Kohomoto [25].

From the contour levels in classical phase space (Fig.12) it becomes clear that the model is related to a classical pendulum. In each unit cell of phase space we have closed classical orbits at small energies. At high energies we see extended contours giving rise to rotating solutions. The parameter k is the analogue of the gravitational constant in the usual pendulum and controls the onset of rotating solutions. The parameter ε interpolates between the discrete Mathieu model ($\varepsilon = 0$) with flux $\Phi' = 2\Phi$ and rescaled energy $E' = kE$ and the quantum integral ($\varepsilon = 2$). Here, we used the algebra homomorpism

$$\Phi \mapsto 2\Phi \quad T_1 \mapsto e^{i\phi/2} {T_2}^* {T_1}^* \quad T_2 \mapsto e^{i\phi/2} T_1 {T_2}^* \tag{82}$$

In the limit $k \to 0$ the term $1/k$ dominates and the system turns into a discrete Laplacian (up to the factor $1/k$). Finally, if $\varepsilon = k$, the Hamiltonian converges in the limit $\varepsilon \to \infty$ to the Hamiltonian of a triangular lattice model with rescaled energy.

Qualitative properties of the spectrum follow again from symmetries of the classical symbol (Table 6) due to Chambers relation (108, section 5).

The discussion of this model will be continued in the next section.

5 Spectra and Eigenfunctions

The analysis of the spectra for Hamiltonians of the Hofstadter type models is greatly simplified by Chambers relation. It expresses the fact that the characteristic polynomial of the Hamiltonian restricted to a fiber over the Brillouin torus is the sum of two terms. The first one is a universal polynomial, i.e., it is independent of the coordinate θ of the Brillouin zone, and the second term is the zeroth order term of the polynomial. It is the only term where the θ-dependence enters. This term is furthermore a scaled version of the principal symbol of the Hamiltonian.

We explain Chambers relation for the case of the Doubly-discrete Quantum Pendulum and prove the following result:

Theorem 1: If the flux $\not\Phi = \frac{p}{q}$ is rational and p, q relatively prime, then the secular determinant for the Doubly-discrete Quantum Pendulum is given by Chamber's formula

$$\det\left(H_{QP}\ (\theta) - z\right) = p(z) + h_{QP}\ (\theta) \tag{83}$$

where $p(z)$ is a polynomial of degree q and

$$\begin{aligned} h_{QP}\ (\theta) &= -4\ T_q(-\varepsilon/2)\left(\cos q\theta_1 + \cos q\theta_2\right) + \\ &+\ 2(-1)^p\left(k^q \cos q\left(\theta_1+\theta_2\right) + \frac{1}{k^q}\cos q\left(\theta_1-\theta_2\right)\right). \end{aligned} \tag{84}$$

Here T_q denotes the Chebyshev polynomial of degree q, defined by $T_q(\cos x) = \cos qx$ and $T_q(-1) = (-1)^q$.

Chambers relation is not only very usefull to compute spectra. It shows also several conceptually interesting features. The offset function $h_{QP}\ (\theta)$ - which is almost the classical symbol - generates on the Brillouin torus a Hamiltonian vector field, which gives rise to a isospectral flow [47]. Furthermore the secular determinant for the Hofstadter model can be factorised at the band edges. This makes it possible to compute the spectral bands algebraically for rather large values of p and q in the field of the cyclotomic extensions of the rationals [8].

Proof: The characteristic polynomial is a function of $\theta \in \mathcal{B}$ and $z \in \mathbb{C}$,

$$F(\theta, z) := \det\left(H_{QP}\ (\varepsilon, k, \theta) - z\right). \tag{85}$$

By definition it is 2π-periodic in the variable θ. Due to Remark 3 after Theorem 2 in Section III it is, however, $\frac{2\pi}{q}$-periodic in θ_1 and θ_2. Hence, it can be expressed in terms of a Fourier series as follows,

$$F(\theta, z) = \sum_{n\in\mathbb{Z}^2} F_n(z)\ \xi_1^{qn_1} \cdot\ \xi_2^{qn_2}, \tag{86}$$

where we introduced the notation $\xi_1 = e^{i\theta_1}$, $\xi_2 = e^{i\theta_2}$.

Next we argue that the only nonvanishing terms in the above Fourier series are those for which $\mid n_1 \mid \ \leq\ 1$ and $\mid n_2 \mid \ \leq\ 1$. This follows from the explicit form of the Hamiltonian,

$$\begin{aligned} H_{QP}\ (\varepsilon, k, \theta) &= \varepsilon \left(\xi_1\ t_1 + \xi_2\ t_2 + \frac{1}{\xi_1}\ t_1^* + \frac{1}{\xi_2}\ t_2^* \right) + \\ &+\ k \left(\xi_1\ \xi_2\ W(1,1) + \frac{1}{\xi_1\ \xi_2}\ W(1,1)^* \right) + \\ &+\ \frac{1}{k} \left(\frac{\xi_1}{\xi_2}\ W(1,-1) + \frac{\xi_2}{\xi_1}\ W(1,-1)^* \right) \end{aligned} \tag{87}$$

and the obvious fact that the determinant is homogeneous of order q in the entries of the $q \times q$ matrix ; so we get

$$F(\theta, z) = \sum_{\substack{\mid n_1 \mid\ \leq\ 1 \\ \mid n_2 \mid\ \leq\ 1}} F_n(z)\ \xi_1^{qn_1}\ \xi_2^{qn_2}\ . \tag{88}$$

The coefficients $F_n(z)$ are now computed by taking limits in this equation to various singular points,

$$\begin{aligned} \det\left(H_{QP}\ (\varepsilon, k, \theta) - z\right) &= \det\Bigg(\varepsilon \left(\xi_1\ t_1 + \xi_2\ t_2 + \frac{1}{\xi_1}\ t_1^* + \frac{1}{\xi_2}\ t_2^* \right) + \\ &+\ k \left(\xi_1\ \xi_2\ e^{-i\Phi/2}\ t_1\ t_2 + \frac{1}{\xi_1\ \xi_2}\ e^{i\Phi/2}\ t_2^*\ t_1^* \right) + \\ &+\ \frac{1}{k} \left(\frac{\xi_1}{\xi_2}\ e^{i\Phi/2}\ t_1\ t_2^* + \frac{\xi_2}{\xi_1}\ e^{-i\Phi/2}\ t_2\ t_1^* \right) - z \Bigg) \\ &= \sum_{\substack{\mid n_1 \mid\ \leq\ 1 \\ \mid n_2 \mid\ \leq\ 1}} F_n\ (z)\ \xi_1^{qn_1}\ \xi_2^{qn_2} \end{aligned} \tag{89}$$

Consider, for instance, the case $\xi_1 \to \infty$. It leads to the equation (using $\det t_1 = 1$)

$$\begin{aligned} &\det\ \left(\varepsilon\ t_1 + k\ \varepsilon_2\ e^{-i\Phi/2}\ t_1\ t_2 + \frac{1}{k\xi_2}\ e^{-i\Phi/2}\ t_1\ t_2^* \right) = \\ &\det\ \left(\varepsilon + k\ \xi_2 e^{-i\Phi/2}\ t_2 + \frac{1}{k\xi_2} e^{i\Phi/2}\ t_2^* \right) = \\ &F_{1,0}(z) + F_{1,1}(z)\ \xi_2^q + F_{1,-1}^{(z)}\ \xi_2^{-q}. \end{aligned} \tag{90}$$

A second limiting procedure $\xi_2 \to \infty$ leads to

$$\det\left(k\ e^{-i\Phi/2} t_2\right) = F_{1,1}(z) \tag{91}$$

Since $\det(t_1) = \det(t_2) = 1$ we get the result

$$\begin{aligned} F_{1,1}(z) &= k^q\ \cdot\ e^{-iq\Phi/2} \\ &= k^q(-1)^p \end{aligned} \tag{92}$$

If we replace the limit above by $\xi_2 \to 0$ we find

$$F_{1,-1}(z) = k^{-q}(-1)^p. \tag{93}$$

Similarly we can replace the limit $\xi_1 \to \infty$ by $\xi_1 \to 0$ followed by $\xi_2 \to \infty$ and $\xi_2 \to 0$. This leads to

$$\begin{aligned} F_{-1,1}(z) &= k^{-q}(-1)^p \\ F_{-1,-1}(z) &= k^q(-1)^p. \end{aligned} \tag{94}$$

Among the coefficients arising in these equations, only $F_{1,0}(z)$ remains to be computed. This follows easily from the

Proposition 2: for any $z \in \mathbb{C}$, $j = 1,2$ and $\lambda \in \mathbb{C} \setminus \{0\}$

$$\det\left(\lambda t_j + \frac{1}{\lambda}\ t_j^* - z\right) = -2\ P_q\left(\frac{z}{2}\right) + (\lambda^q + \lambda^{-q}) \tag{95}$$

where $T_n(x) = \cos(n \arccos(x))$ is the n-th Chebyshev polynomial.

The proof of the proposition uses again the same idea as before. The function $\det\left(\lambda t_1 + \frac{1}{\lambda}\ t_1^* - z\right)$ is a Laurent polynomial in λ of order q and invariant under the substitution $\lambda \to e^{\frac{2\pi i}{q}} \lambda$. Hence, it can be expressed in terms of a Fourier series with three terms only,

$$\det\left(\lambda t_1 + \frac{1}{\lambda}\ t_1^* - z\right) = b_0(z) + b_{+1}(z)\lambda^q + b_{-1}(z)\lambda^{-q}. \tag{96}$$

The terms $b_{\pm 1}(z)$ can be computed through the limits $\lambda \to \pm\infty$ from which we infer that $b_\pm(z) = \det t_1^{\pm 1} = 1$. So are left with the computation of the polynomial $b_0(z)$.

By construction t_1 has the eigenvalue one and is diagonal. Hence, the left-hand side of (96) vanishes if

$$\lambda + \frac{1}{\lambda}\ - z = 0. \tag{97}$$

From this equation and (96) we conclude that

$$b_0\left(\lambda + \frac{1}{\lambda}\right) + \lambda^q + \lambda^{-q} = 0 \tag{98}$$

which up to trivial factors, is the functional equation for the Chebyshev polynomial $T_q(x)$,

$$T_q\left(\frac{1}{2}\ \left(\lambda + \lambda^{-1}\right)\right) - \frac{1}{2}\ (\lambda^q + \lambda^{-q}) = 0. \tag{99}$$

So, we finally get the result

$$b_0(x) = -2\ P_q\left(\frac{x}{2}\right). \tag{100}$$

This proves Proposition 2.

Now we are prepaired to compute F_{10} from equation (90):

$$\begin{aligned} F_{10}(z) &= \det\left(\varepsilon + k\ \xi_2\ e^{-i\Phi/2}\ t_2 + \frac{1}{k\ \xi_2}\ e^{i\Phi/2}\ t_2^*\right) - \\ &- k^q(-1)^p\left(\xi_2^q + \xi_2^{-q}\right) \\ &= -2\ P_q\left(-\frac{\varepsilon}{2}\right). \end{aligned} \tag{101}$$

Analogously, we obtain

$$F_{-1,0}(z) = -2\ P_q\left(-\frac{\varepsilon}{2}\right). \tag{102}$$

The only term left is $F_{00}(z)$. The results proved so far show that it is the only coefficient among the F_n's which possibly has an explicit z-dependence. All other terms are independent of z. Summarizing we obtain

$$\begin{aligned} F(\theta, z) &= F_{(0,0)}(z) + \sum_{\substack{|\ n_1\ | = 1 \\ |\ n_2\ | = 1}} (-1)^p\ k^{n_1 n_2 q}\ \xi_1^{n_1 q}\ \xi_2^{n_2 q}\ - \\ &- \ 2\ T_q\left(-\varepsilon/2\right)\left(\left(\xi_1^q + \xi_1^{-q}\right) + \left(\xi_2^q + \xi_2^{-q}\right)\right). \end{aligned} \tag{103}$$

This finishes the proof of theorem 1.

Similar results hold for many other Hamiltonians of the Hofstadter type; in particular, for all those which are of the form

$$H = \sum_{\substack{|\ m_1\ | \le 1 \\ |\ m_2\ | \le 1}} t(m)\ W(m) \tag{104}$$

This class contains all the models mentioned so far.

For rational flux the spectrum of the Hamiltonian is computed in terms of band functions, defined as follows. For $\not{\Phi} = \frac{p}{q}$, $p \wedge q = 1$, the Hamiltonian H may be expressed in terms of a direct integral (Section 3, Theorem 3 and Eq.(63)

$$H \ \cong\ \frac{1}{|\mathcal{B}|} \int_{\mathcal{B}}^{\oplus} d^2\theta H(\theta) \otimes \mathbb{1} \tag{105}$$

where $H(\theta)$ is a $q \times q$ matrix operator. Its spectrum is given in terms of the spectra of the fiber Hamiltonians, $H(\theta)$, by

$$\sigma(H) \ =\ \bigcup_{\theta \in \mathcal{B}} \sigma(H(\theta))\ . \tag{106}$$

The latter is computed as the zero set of the secular determinant:

$$\{z \mid \det\ (H(\theta) - z) = 0\} = \{E_1(\theta), \dots, E_q(\theta)\}. \tag{107}$$

$E_1(\theta), \ldots, E_q(\theta)$ are the band functions. Since $H(\theta) = H(\overline{\theta})^*$ is analytic in θ_1 and θ_2 the band functions are real–analytic in both θ_1 and θ_2 seperately) and continuous jointly in θ_1 and θ_2 [35].

Due to Chambers relation,

$$\det(H(\theta) - z) = P(z) - h(\theta) \tag{108}$$

the band functions are the branches of the relation $P^{-1} \circ h$.

Each band function $E(\theta)$ gives rise to a band $[E_{\min}, E_{\max}] \subset \sigma(H)$, where the band edges are critical points, $dE(\theta_{min}) = dE(\theta_{max}) = 0$.

Chamber's relation has another interesting consequence for the critical points of all band functions. Every critical point of the classical symbol $h(\theta)$ is a joint critical point of all band functions since

$$P'(E(\theta)).E'(\theta) = h'(\theta). \tag{109}$$

The converse is slightly more subtle. If $E(\theta)$ describes a band which does not touch another one, i.e., $P'(E(\theta)) \neq 0$, for critical points θ of h, the critical points of $E(\theta)$ coincide with those of $h(\theta)$. Degeneracies of spectra occur generically only on a set of codimension 3, hence for discrete points (θ, Φ) in $\mathcal{B} \times \mathbb{R}$ (v. Neumann and Wigner [48]).

Notice that the fact just mentioned simplyfies the computation of spectra considerably since instead of computing all the band functions one merely needs to compute the band edges i.e. the zeros of the equation

$$P(z) = h(\theta_{crit}) \tag{110}$$

for all critical points θ_{crit} of h.

Critical points of band functions or of the corresponding classical symbol, respectively, are relevant for the semiclassical analysis of the spectra (see below). They can have a complicated geometrical structure depending on the parameters of the model.

As an example we consider the case of the Doubly-discrete Quantum Pendulum. The parameter space is decomposed into five regions A to E as shown in Fig. 13. In Table 7 we list the critical sets in the Brillouin torus $\mathcal{B}$ of the classical symbol. a max and a min denote absolute maxima and absolute minima respectively, while max and min refer to local maxima and minima.

In all five regions, there is just one absolute maximum at $(x_1, x_2) = (0, 0)$. In a vicinity of this point the Hamiltonian is parabolic and gives rise to oscillating classical solutions. There is one absolute minimum in all regions except in case C where $\varepsilon = 2$. This case is the one originating from discrete geometry. The absolute minimum is a loop in $\mathcal{B}$, hence a classical orbit.

In the general case, there is a saddle point between the absolute maximum and the absolute minimum. This is clearly seen from the plot of classical contour levels (see Fig. 12).

We have computed numerically the band spectrum of the Doubly-discrete Quantum Pendulum for rational flux by diagonalizing the fiber Hamiltonian $H(\theta)$ at the critical points of the dilated classical symbol h_{QP} defined in (84). These values can be computed easily from the critical points of the classical symbol (Table 7). In Figures 14 to 18 we present typical spectra for the regions A to E. In Figures 19 to 22, Husimi functions for various paramters and quantum numbers are shown. The figures contain the classical orbits and show that the Husimi functions are localized at their classical counterparts.

Now we present a semi-rigorous semi-classical analysis of the spectrum of the Doubly-discrete Quantum Pendulum and apply techniques known from the Hofstadter model [50] to the critical points of the classical symbol. If the critical points are not isolated, as is the case for the Doubly-discrete Quantum Pendulum with $\varepsilon = 2$, one has to apply technics which are analytically even more involved [15, 28]. They go back in spirit to the reaction path method of quantum chemistry [42, 19].

In the case of an isolated critical point there are classically oscillating orbits nearby giving rise to quasi modes. Their energy can be computed as follows: Consider e.g.the absolute maximum of the classical symbol at $(x_1, x_2) = (0, 0)$, which is unique for all parameter values. Using a semi-classical representation of the Rotation Algebra namely

$$T_1 = e^{i(x_1 + \sqrt{\Phi} K_1)}, \quad T_2 = e^{i(x_2 + \sqrt{\Phi} K_2)}, \quad [K_1, K_2] \; = \; i \quad , \tag{111}$$

we expand the Hamiltonian in $\sqrt{\Phi}$ around the critical point up to second order and obtain the formal expression

$$H = H_{QP}(0,0) \pm \mid \Phi \mid \sqrt{\det D^2 H_{QP}(0,0)}\, (K_1^2 + K_2^2) + O(|\Phi|^{3/2}). \tag{112}$$

$D^2 H_{QP}(0,0)$ is the Hessian of the classical symbol at the critical point $(0,0)$ where the equation holds:

$$\omega_{\varepsilon,k} = -\sqrt{\det D^2 H_{QP}(0,0)} = \sqrt{(\varepsilon + 2k)(\varepsilon + \frac{2}{k})} \tag{113}$$

and, thus, the semi-classical eigenvalues are given by

$$E_n = 2\,(2\varepsilon + k + \frac{1}{k}) - \omega_{\varepsilon,k}(2n+1), \quad (n \in \mathbb{Z}). \tag{114}$$

In physical terms this corresponds to a Bohr-Sommerfeld quantization of classically oscillating solutions.

This approach is oriented towards energies at the top - respectively for isolated critical values of the classical symbol - and small flux. In this case the bands are very short, so one may refer to them as single numbers. As in other Hofstadter-like, models the results match the exact spectrum very well even for comperatively large values of magnetic flux Φ (see Fig.23). For larger flux and smaller energies this changes - due to tunneling - and the bands get longer.

This semi-classical argument does not hold anymore if the energy is close to a classical saddle point where there are rotating classical solutions.

Except at $\varepsilon = 2$ the classical symbol possesses an absolut minimum in phase space which, again, gives rise to energy levels of the same type as before. This time, however, they emerge from the minimal classical energy. In Fig. 18 (region E) one can easily spot them since the minimal energy is well separated from the separatrix energy, as in the case of the square lattice.

In each region of the parameter space we find rotating solutions for the classical Hamiltonian. In the covering space of phase space they appear as non compact contours in an energy range between two distinct saddle points. Except for the trajectory at minimal energy for $\varepsilon = 2$ we always find two different rotating solutions at the same energy level. Their semiclassical analysis is more complicated and will not be discussed here [15, 28].

6 Acknowledgment

The idea of proof of Chambers relation (Section 5) and much more about the Hofstadte model we learned from Jean Bellissard many years ago, before the discovery of the Doubly-discrete Quantum Pendulum. In particular he introduced us into the algebraic setting of the Hofstadter Model. We benefitted furthermore much from discussions with Ulrich Pinkall and many other members of the SFB "Differential Geometry and Quantum Physics". In particular the automorphism relating the Hofstadter model to the Doubly-discrete Quantum Pendulum is due to him (Section 5). Many stimulating discussions we had with Ludwig Faddeev. Volker Bach helped us with scientific and linguistic questions a like.

This work is supported in part by the DFG, and the Erwin Schrödinger Institute in Vienna, where we acknowledge useful discussion with Paul Wiegmann and Anton Zabrodin.

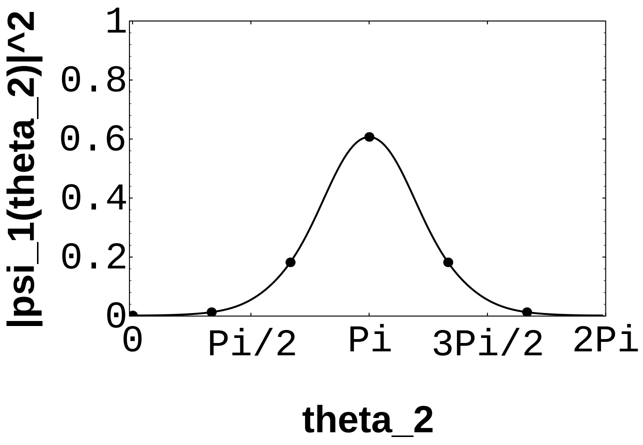

Figure 1: Groundstate of the Discrete Harmonic Oscillator for $q = 6$

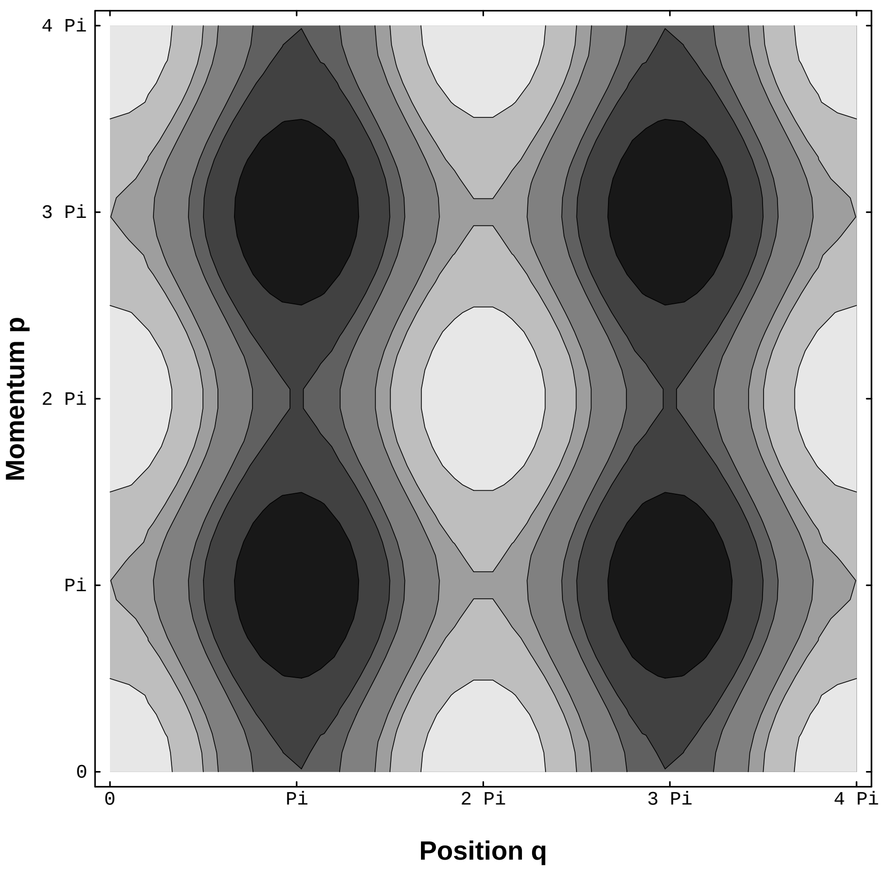

Figure 2: Classical contour levels the the Discrete Mathieu model for $\mu = 0.5$

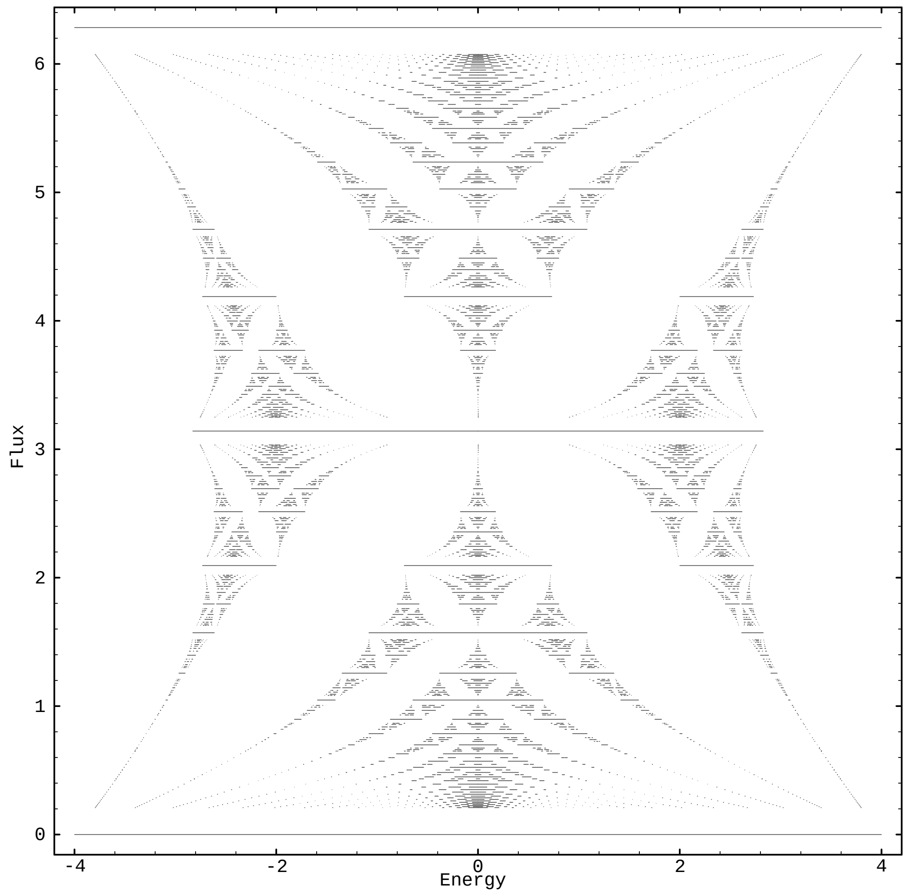

Figure 3: Hofstadter Butterfly: Spectrum of the Hofstadter Model

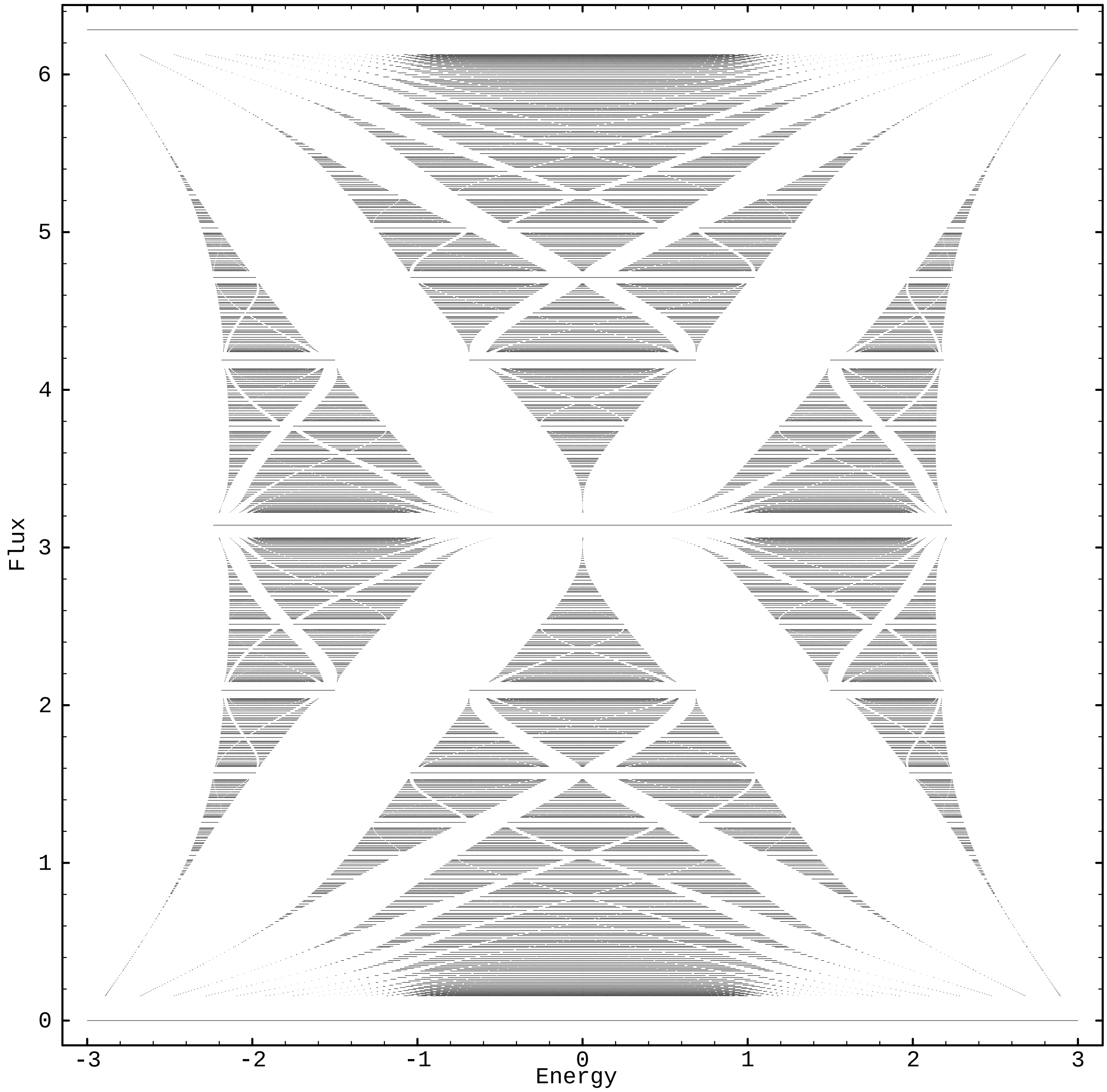

Figure 4: Spectrum of the Discrete Mathieu Hamiltonian for $\mu = 0.5$ and $q < 40$

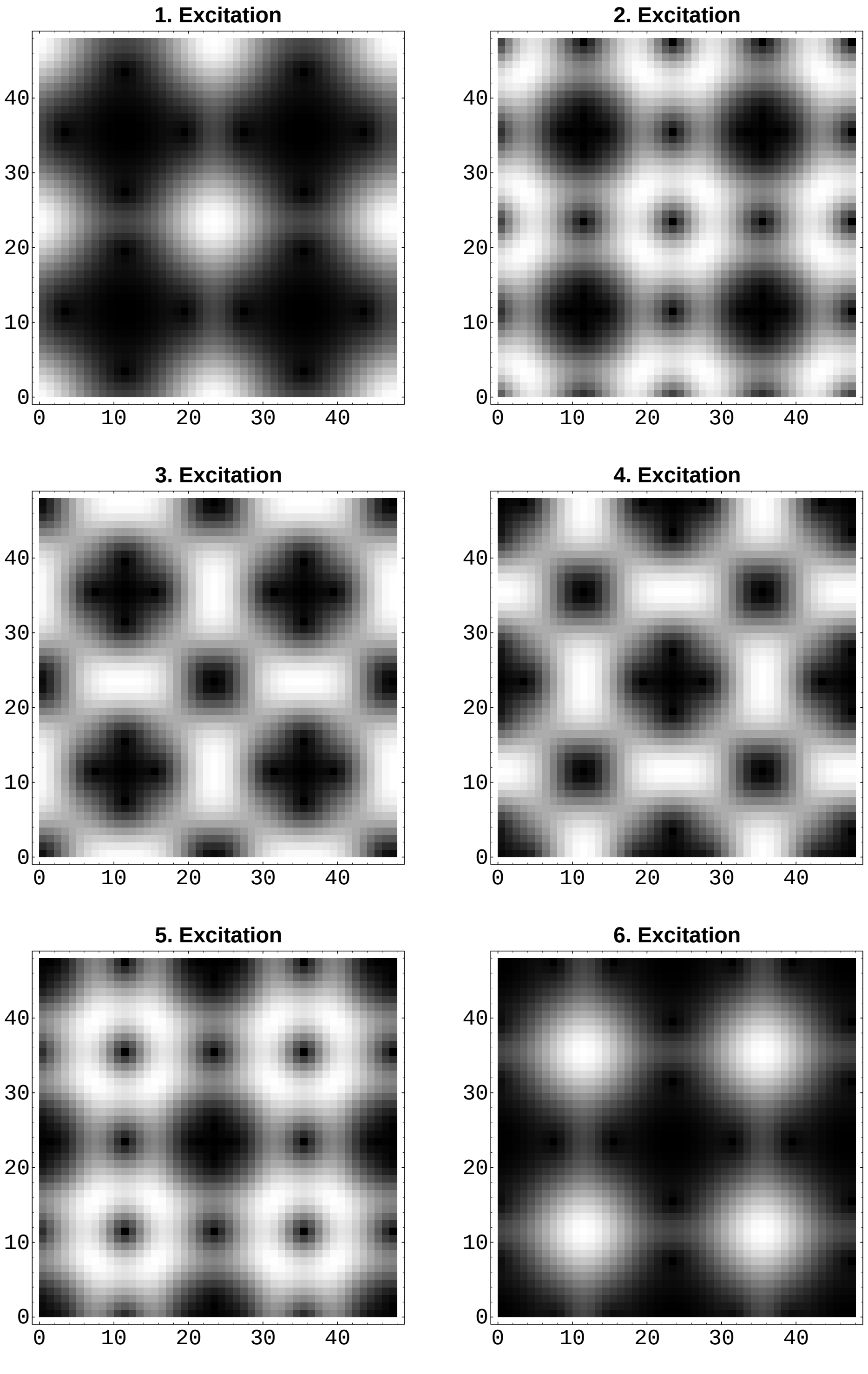

Figure 5: Continuous Husimi Transformation for Hofstadter model ($p/q = 1/6$)

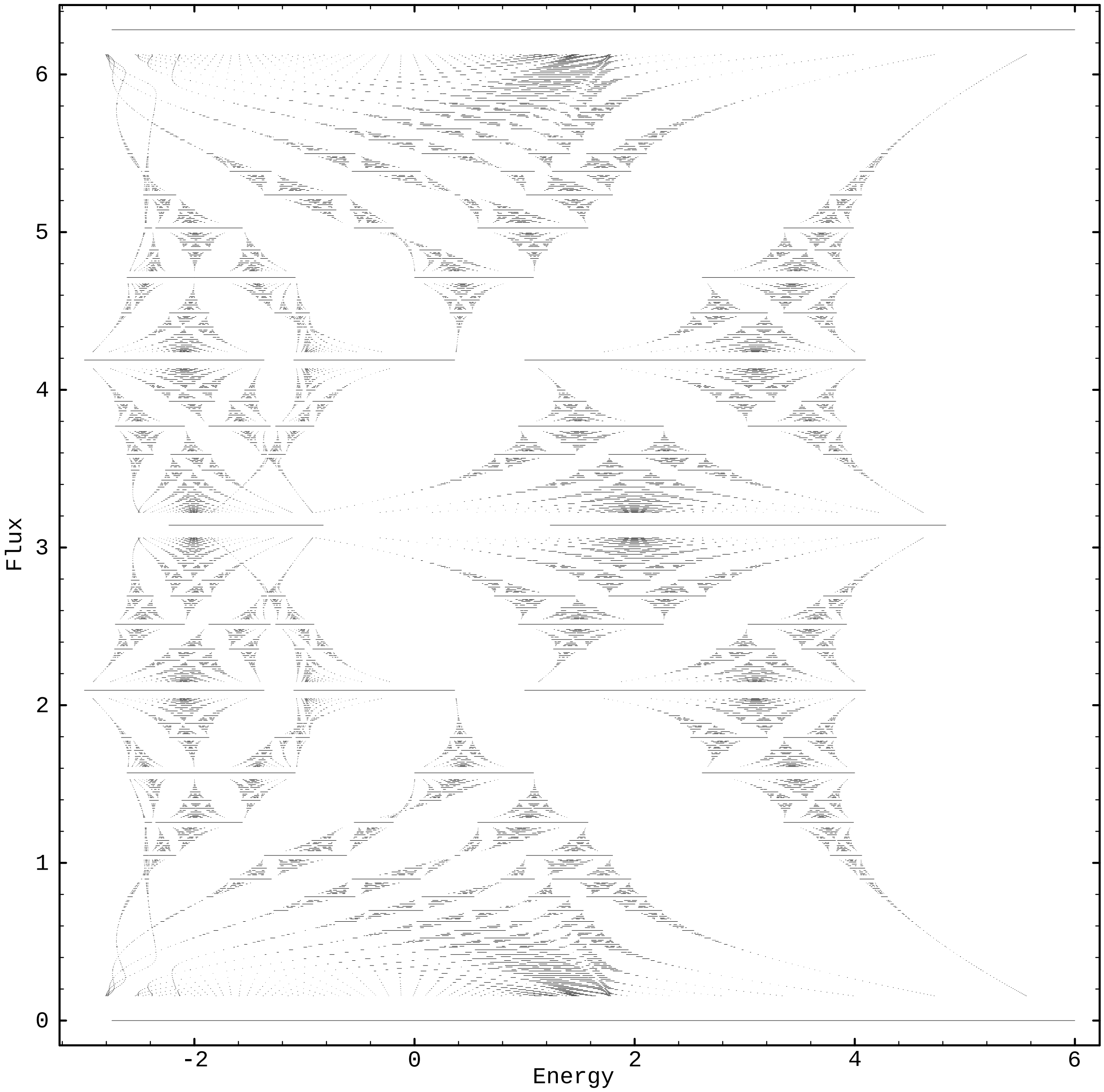

Figure 6: Spectrum of the Second Neighbour Square Lattice model for $\varepsilon = 0.25$ and $q < 40$

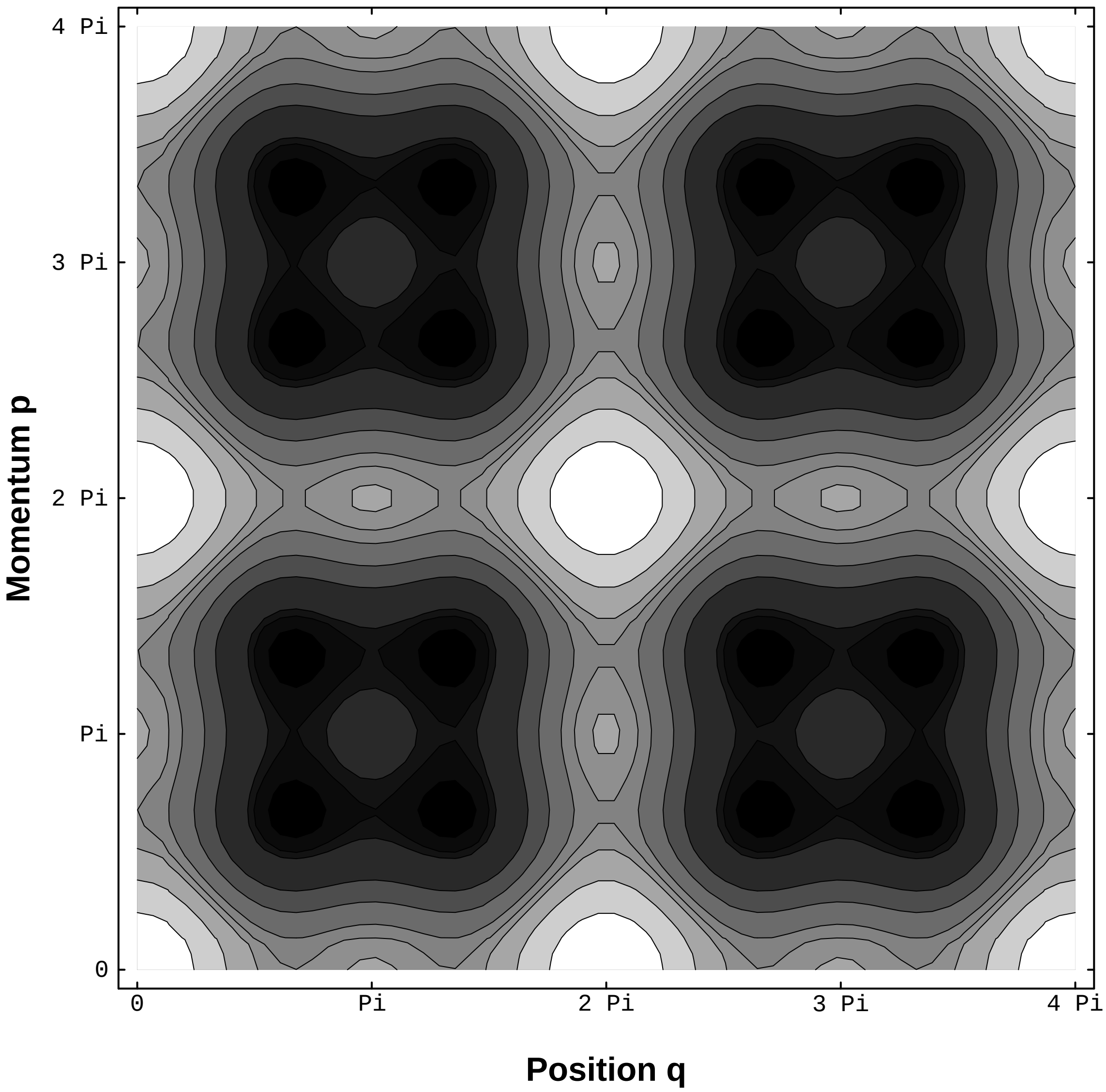

Figure 7: Classical contour levels in Second Neighbour Square Lattice model for $\varepsilon = 0.25$

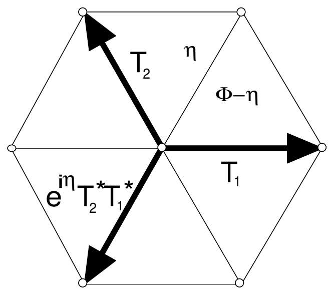

Figure 8: Hopping interaction in the Triangular Lattice model

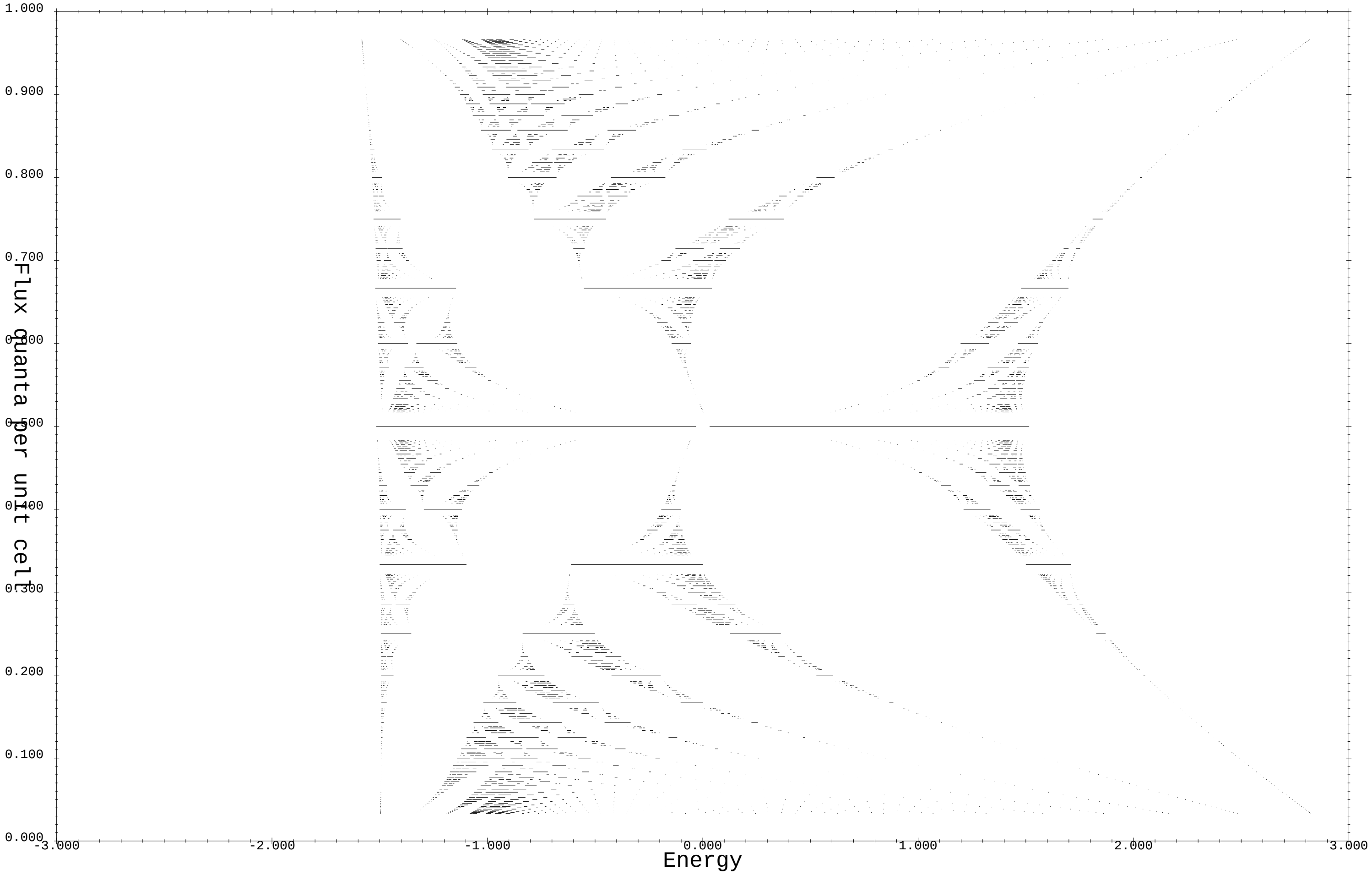

Figure 9: Spectrum of the Triangular Lattice model for $\eta = 0.075$ and $q \leq 40$

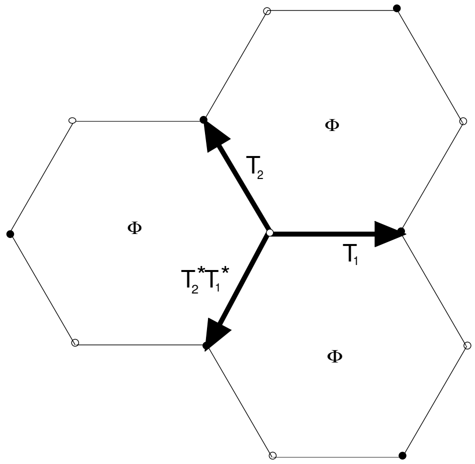

Figure 10: Interactions in the Honeycomb model

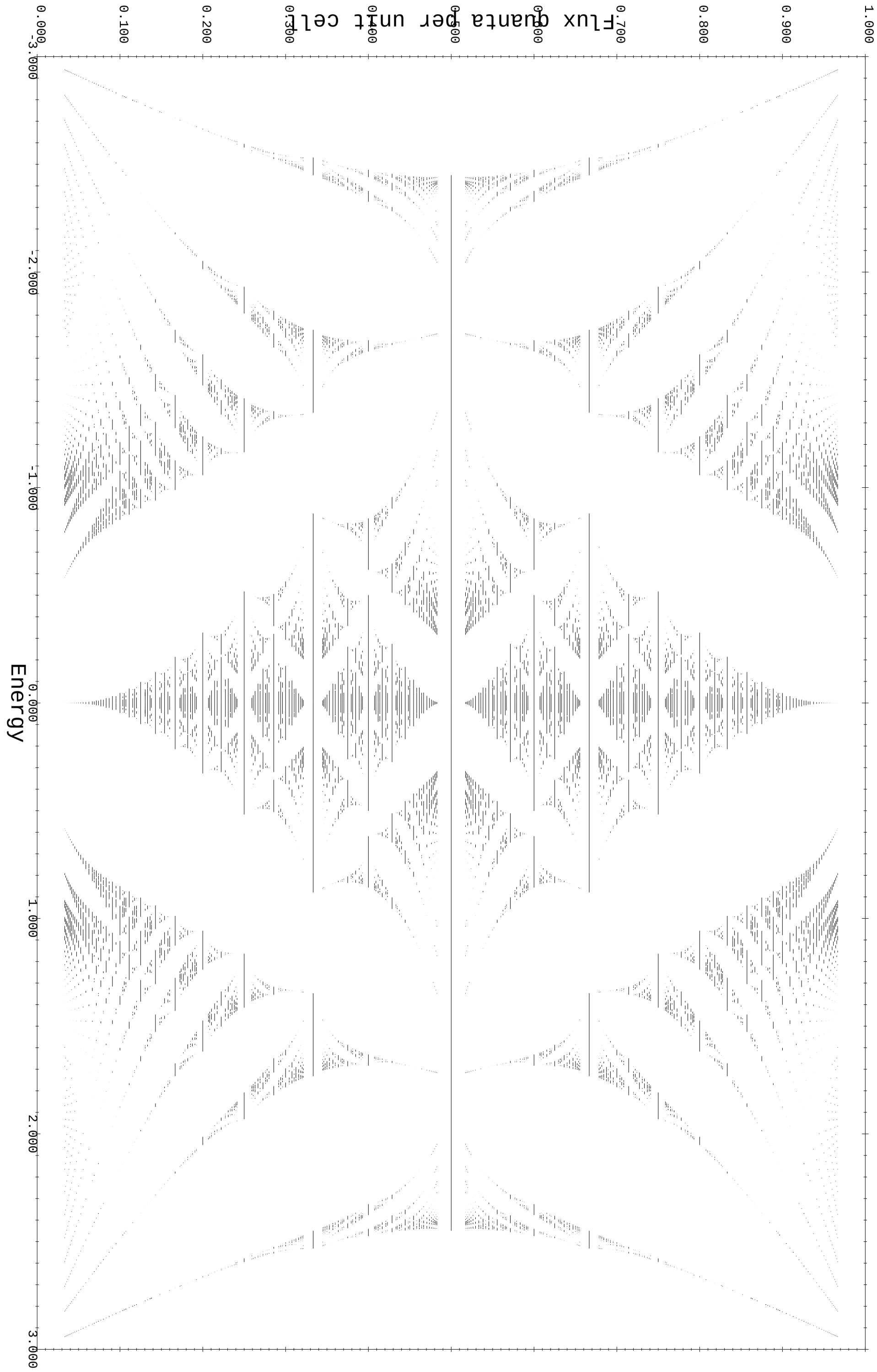

Figure 11: Spectrum for the Honeycomb model

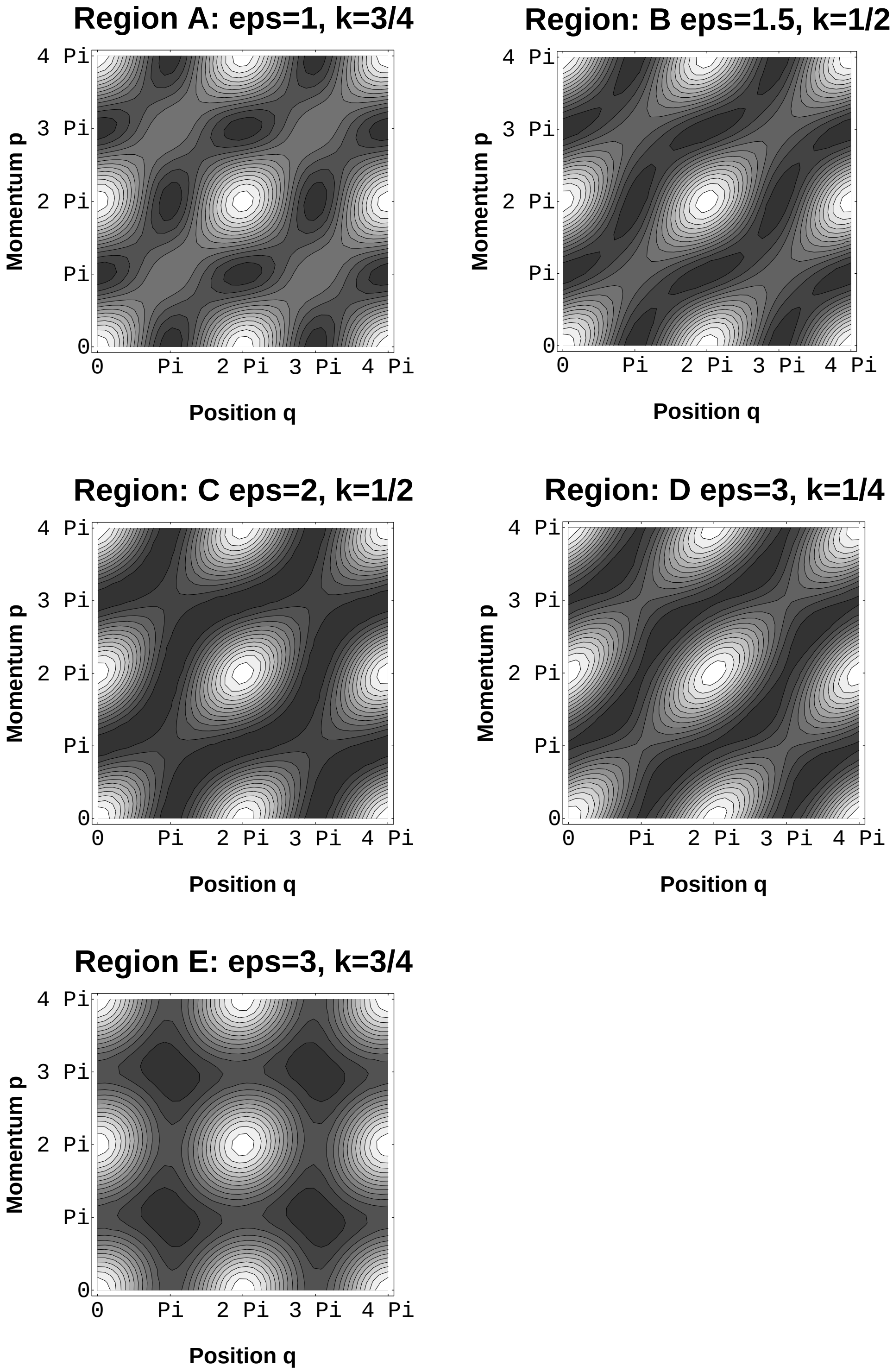

Figure 12: Examples for classical contour levels in regions A to E for the Doubly-discrete Quantum Pendulum

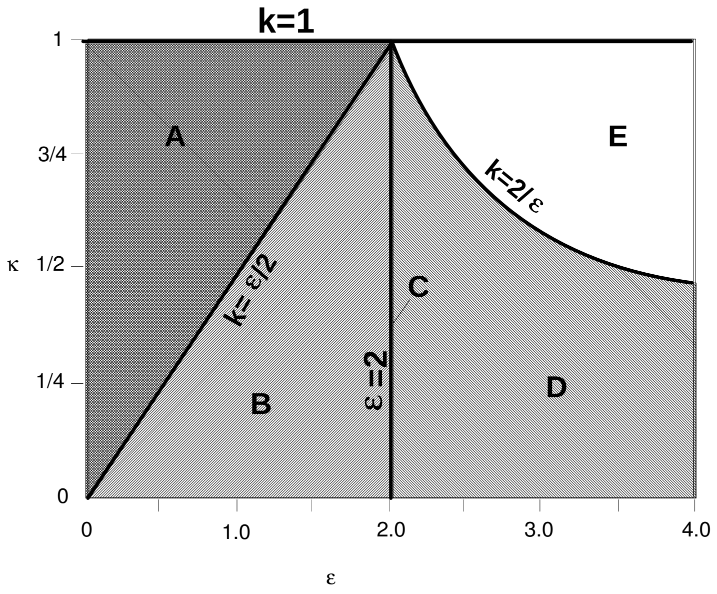

Figure 13: Regions A to E for critical points in parameter space for the Doubly-discrete Quantum Pendulum

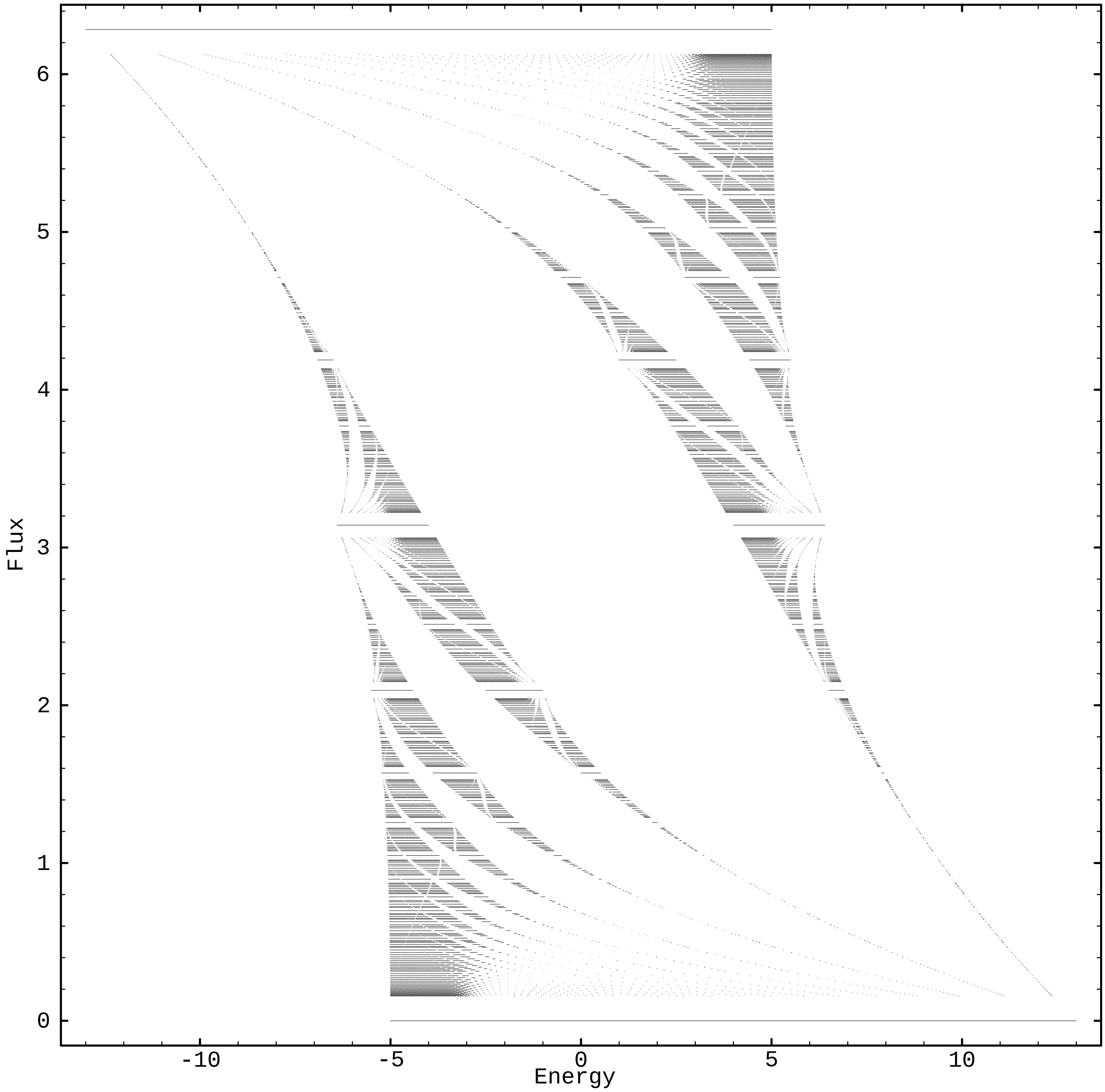

Figure 14: Spectrum of Doubly-discrete Quantum Pendulum at $\varepsilon = 2$ and $k = 1/2$ (Region C)

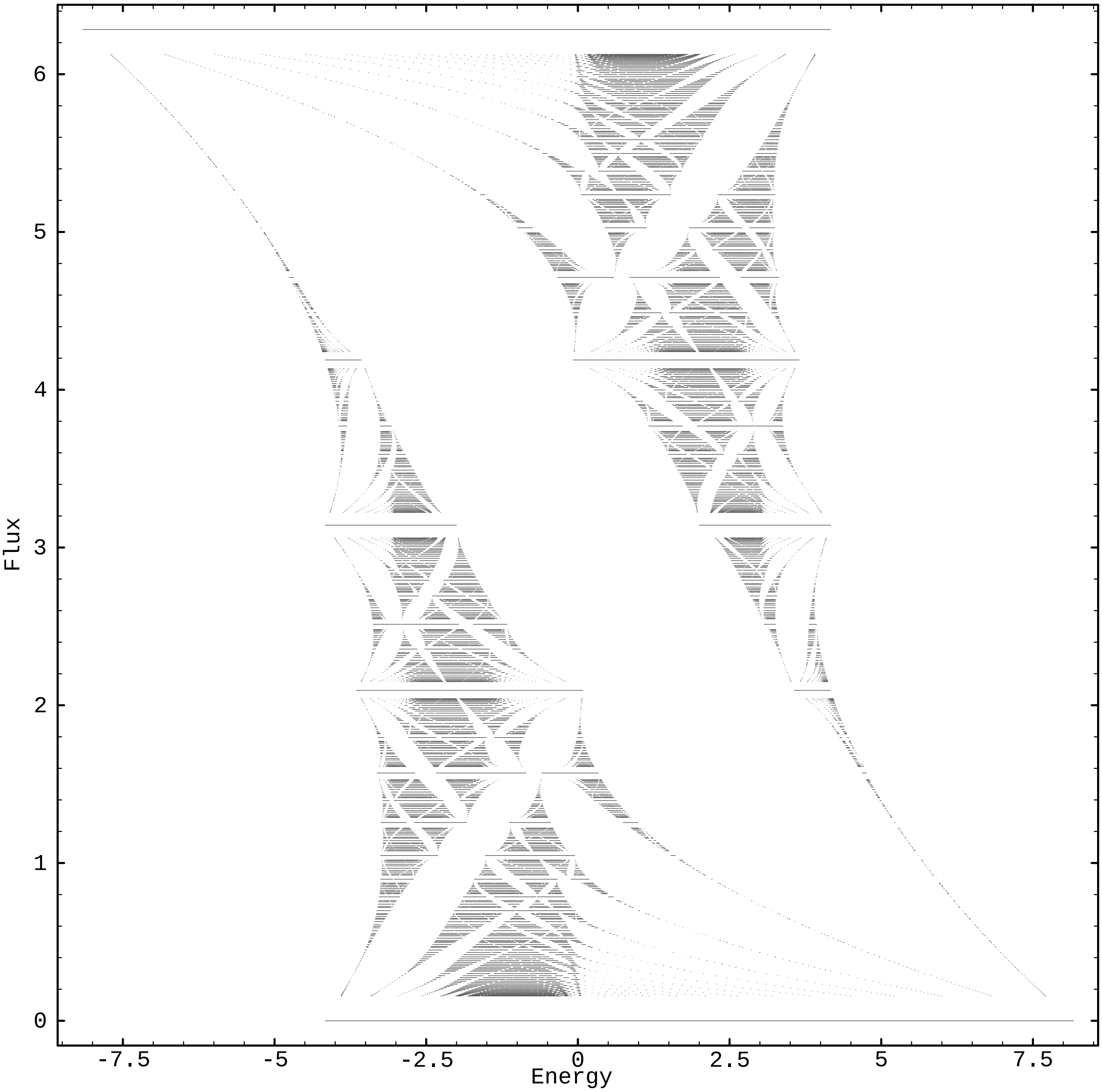

Figure 15: Spectrum of Doubly-discrete Quantum Pendulum at $\varepsilon = 1$ and $k = 3/4$ (Region A)

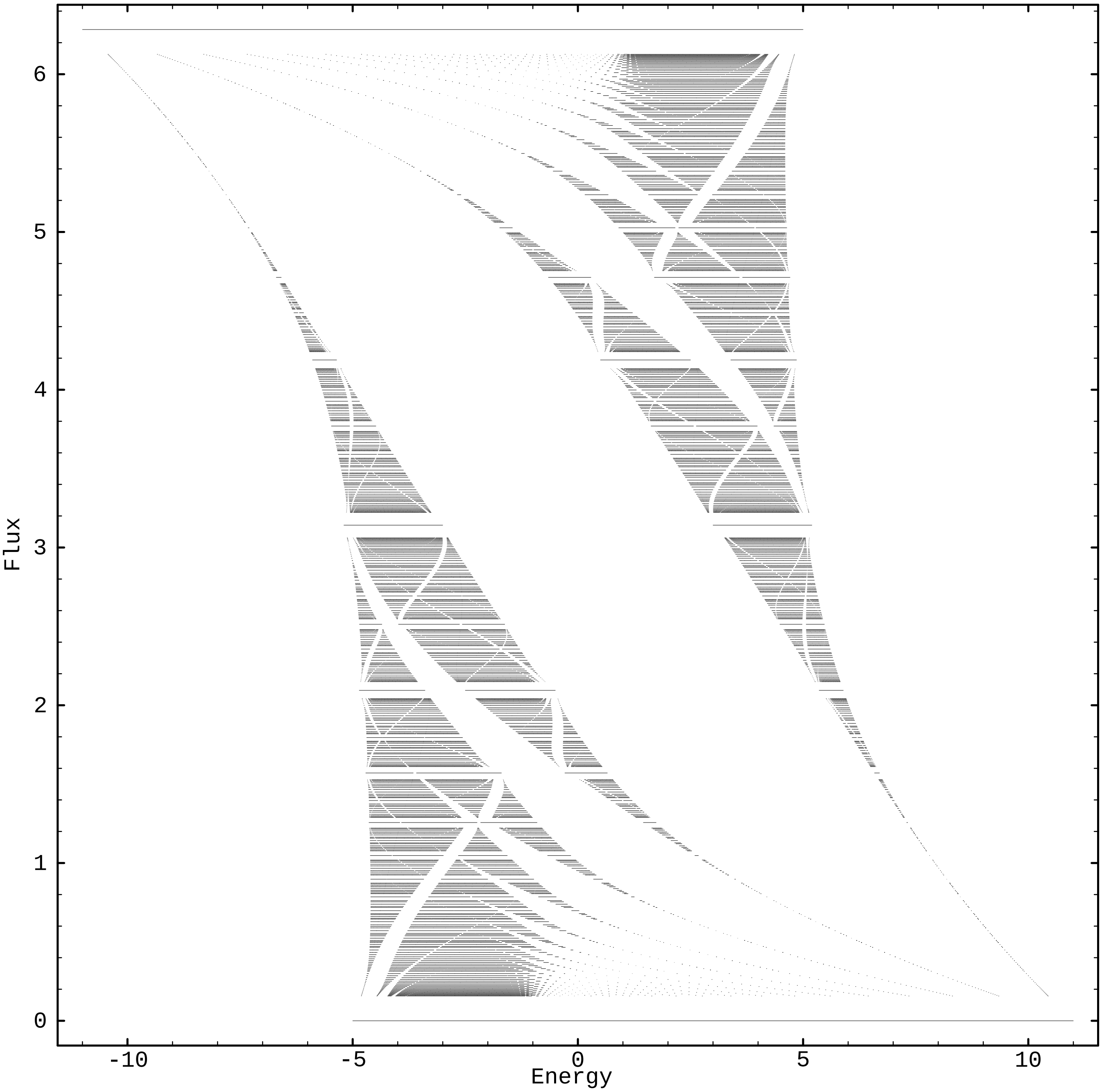

Figure 16: Spectrum of Doubly-discrete Quantum Pendulum at $\varepsilon = 1,5$ and $k = 1/2$ (Region B)

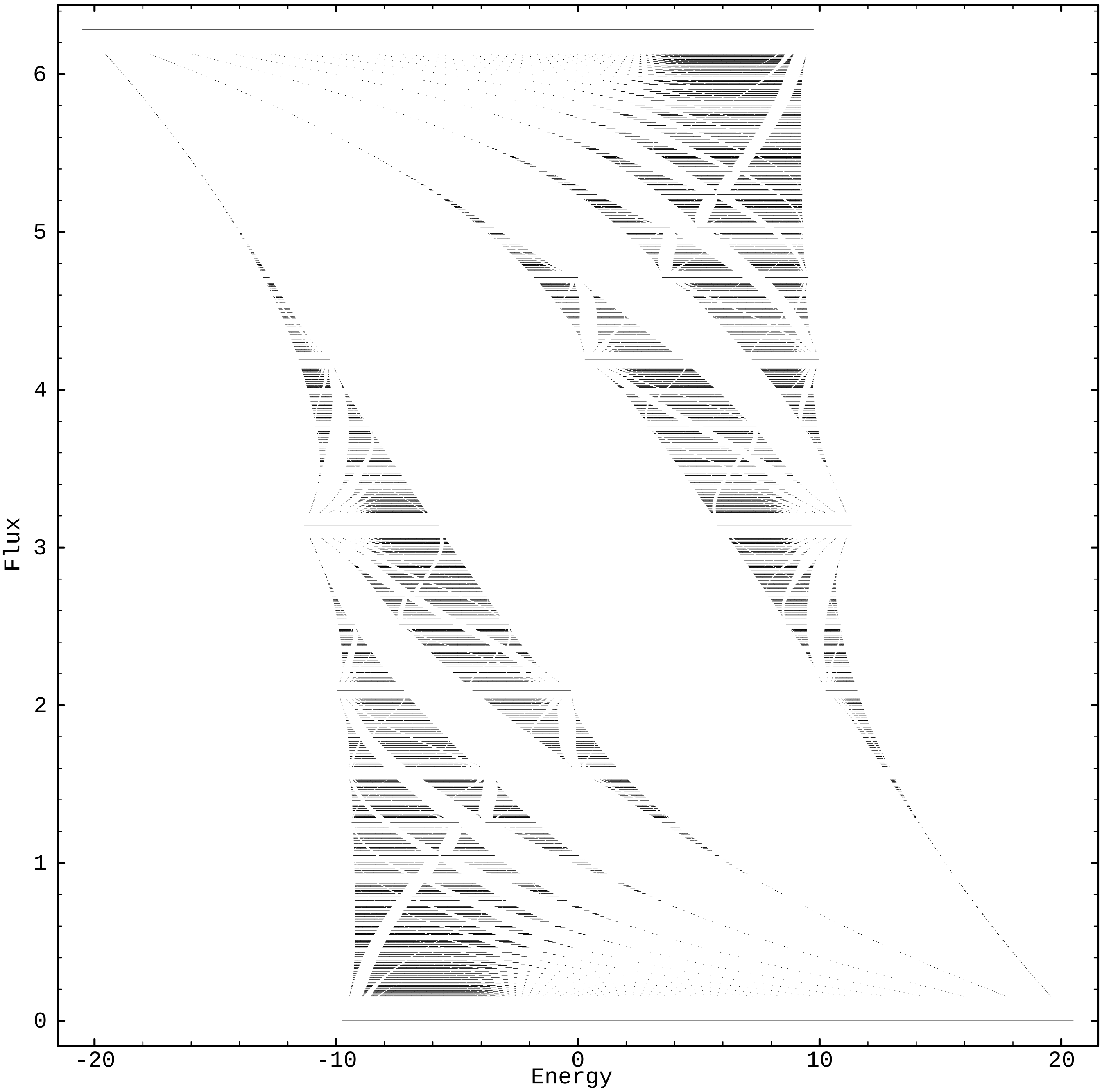

Figure 17: Spectrum of Doubly-discrete Quantum Pendulum at $\varepsilon = 3$ and $k = 1/4$ (Region D)

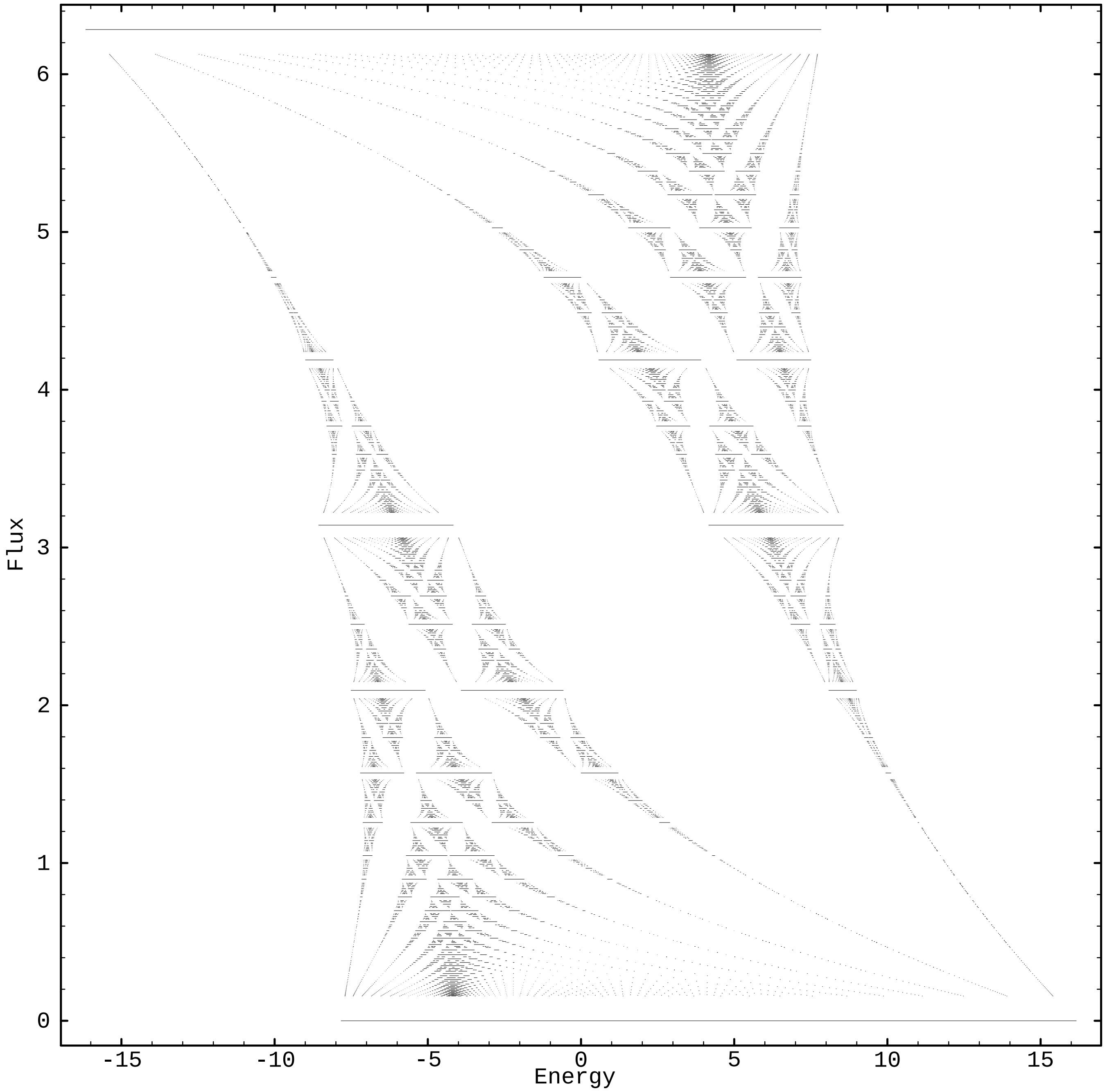

Figure 18: Spectrum of Doubly-discrete Quantum Pendulum at $\varepsilon = 3$ and $k = 3/4$ (Region E)

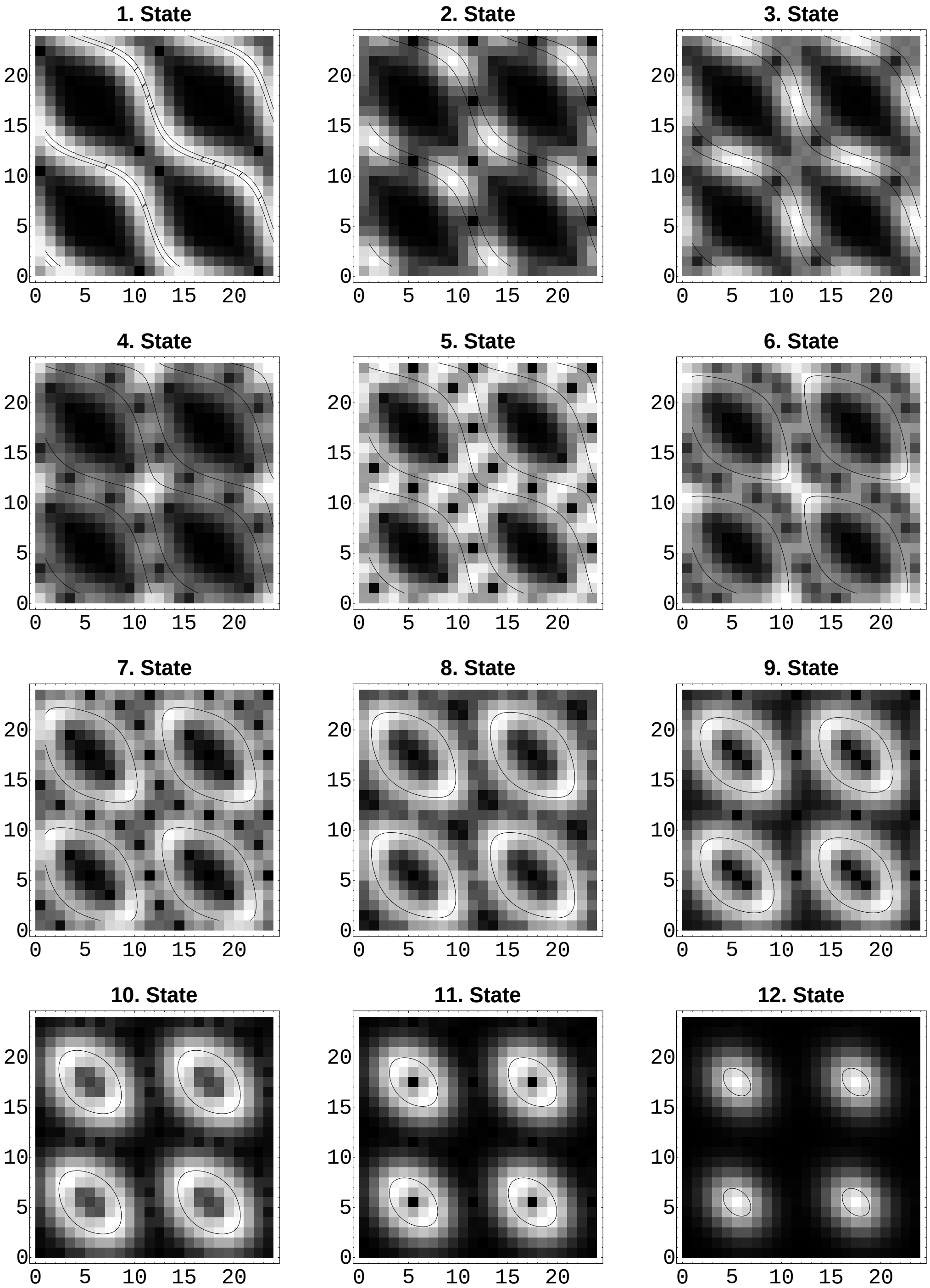

Figure 19: Husimi transfomation for eigenstates of Quantum Pendulum at $\Phi = 2\pi\frac{1}{12}$, $\varepsilon = 2$, $k = 1/2, \theta = (0, 0)$

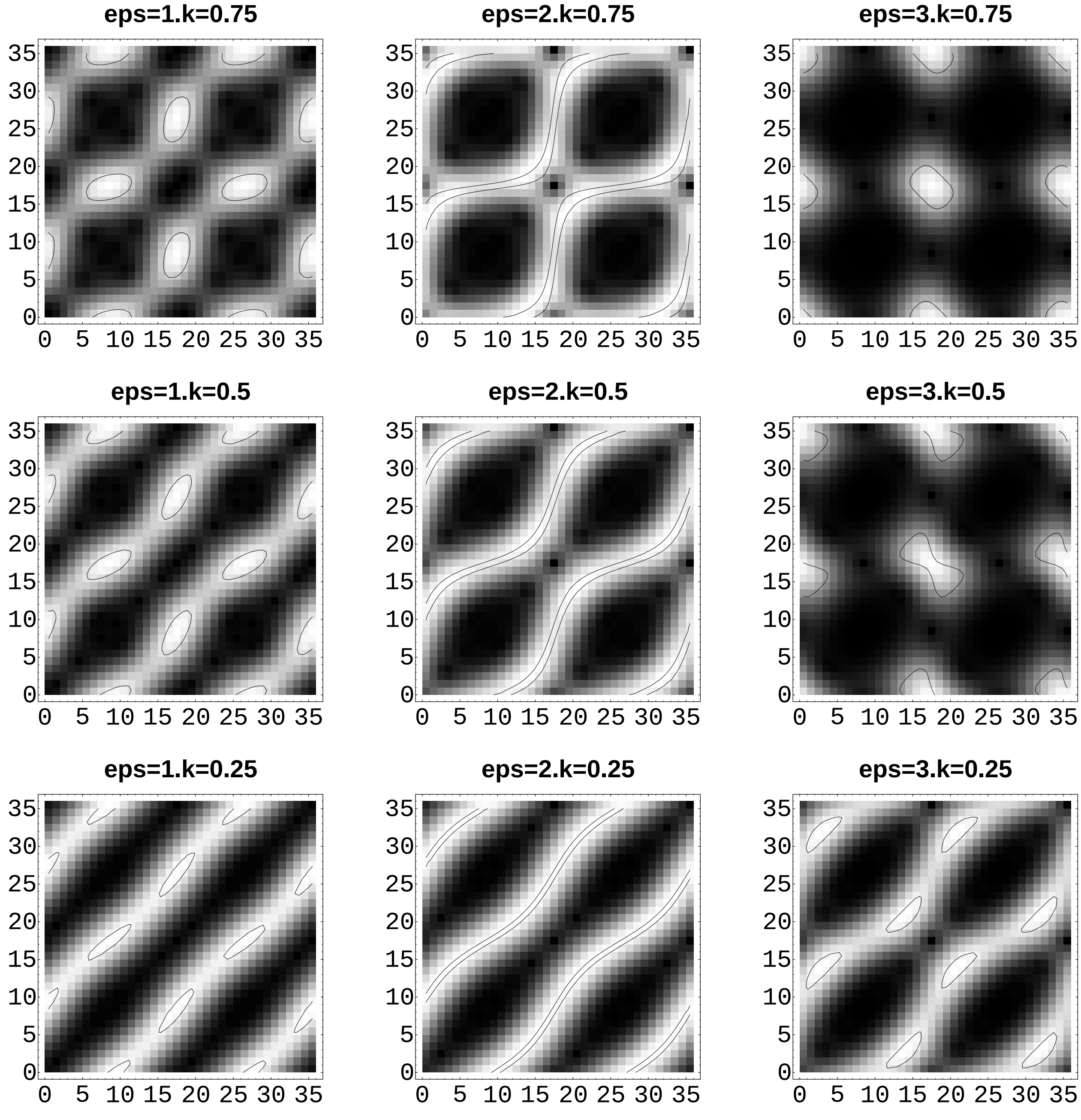

Figure 20: Husimi transfomation of ground state of Doubly-discrtet Quantum Pendulum for $\Phi = 2\pi\frac{1}{9}$

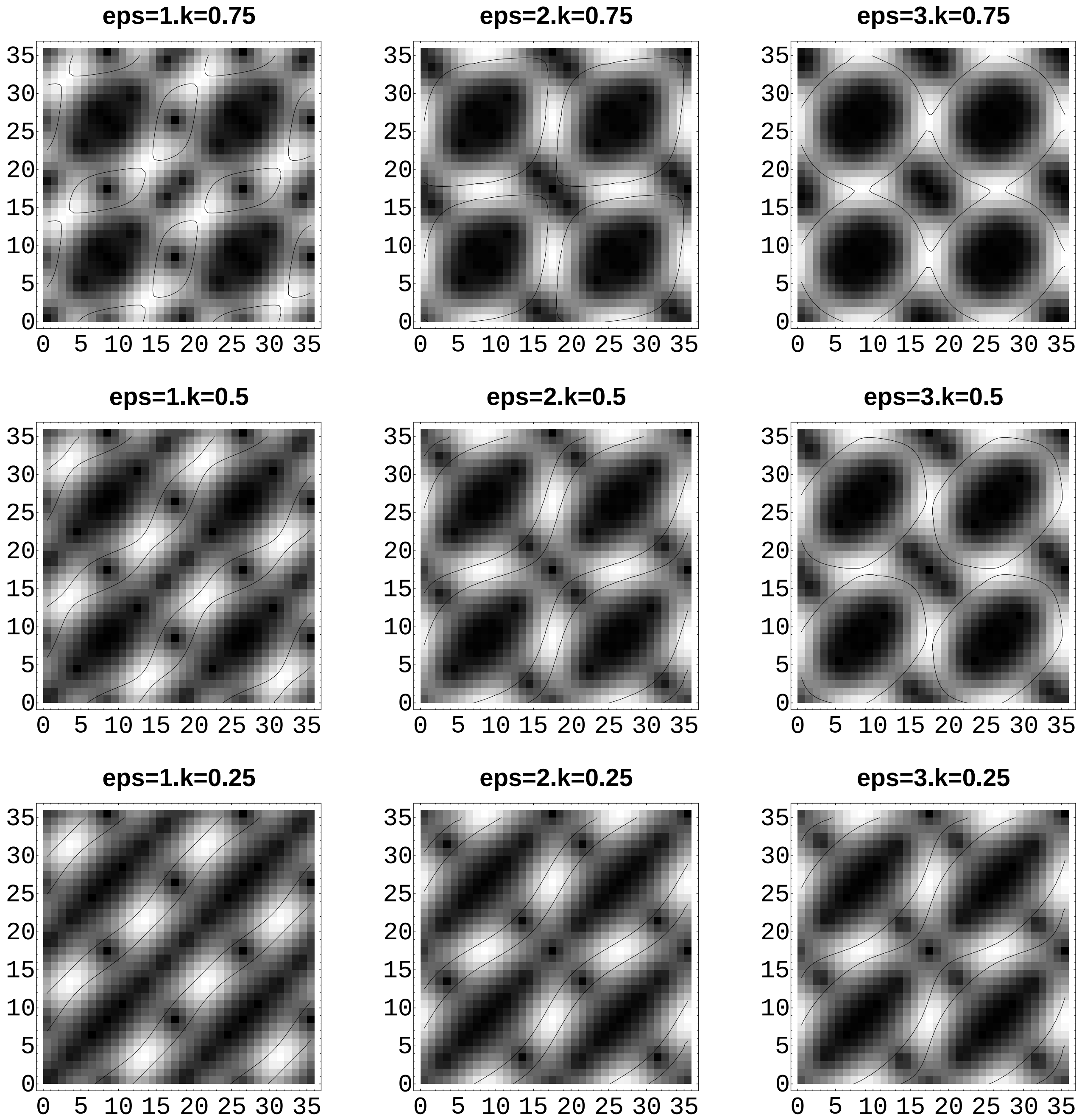

Figure 21: Husimi transfomation of third state of Doubly-discrete Quantum Pendulum for $\Phi = 2\pi\frac{1}{9}$

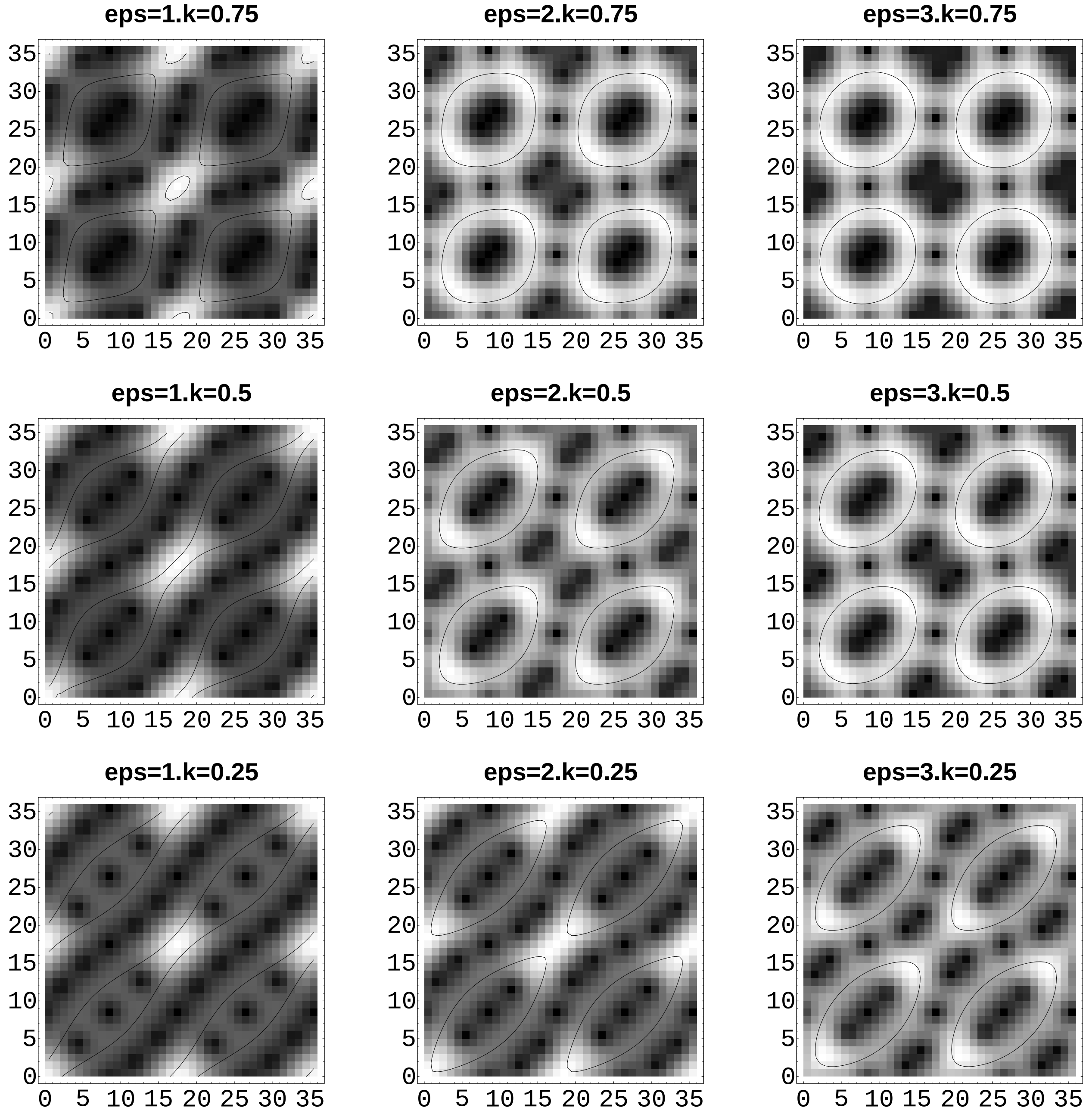

Figure 22: Husimi transfomation of sixth state exitation of Doubly-discrete Quantum Pendulum for $\Phi = 2\pi\frac{1}{9}$

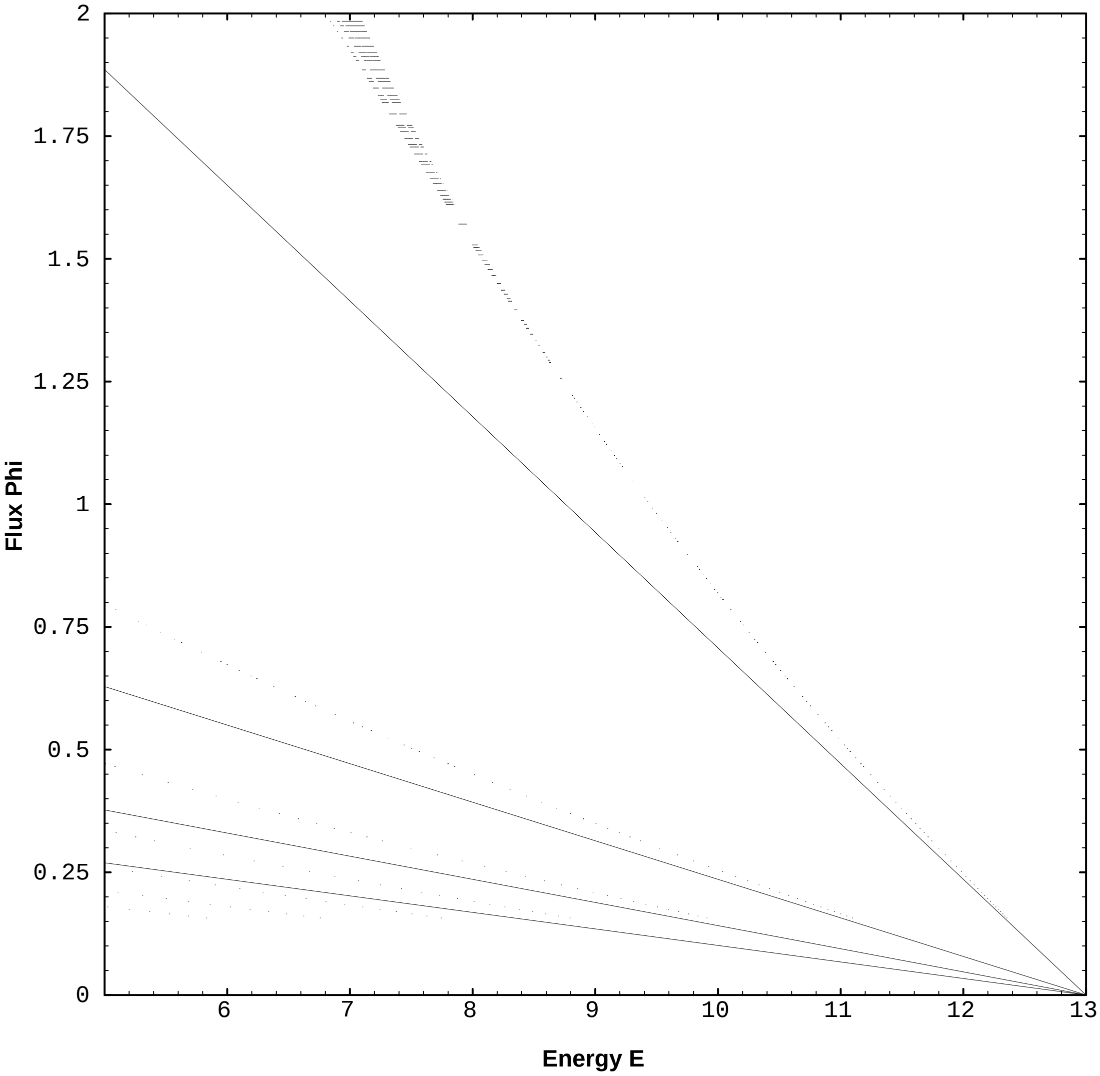

Figure 23: Exact spectrum and semi-classical Landau levels at $\epsilon = 2, k = 1/2$

Nr.	Description	Matrix	$\det(M)$	Automorphism	Classical
i	rotation by $\pi/2$	$\begin{pmatrix} 0 & -1 \\ 1 & 0 \end{pmatrix}$	1	$T_1 \to T_2$ $T_2 \to T_1^\star$	$x_1 \to x_2$ $x_2 \to -x_1$
ii	rotation by π	$\begin{pmatrix} -1 & 0 \\ 0 & -1 \end{pmatrix}$	1	$T_1 \to T_1^\star$ $T_2 \to T_2^\star$	$x_1 \to -x_1$ $x_2 \to -x_2$
iii	reflection at $x_1 = x_2$	$\begin{pmatrix} 0 & -1 \\ -1 & 0 \end{pmatrix}$	-1	$T_1 \to T_2$ $T_2 \to T_1$	$x_1 \to x_2$ $x_2 \to x_1$
iv	reflection at $x_1 = -x_2$	$\begin{pmatrix} 0 & 1 \\ 1 & 0 \end{pmatrix}$	-1	$T_1 \to T_2^\star$ $T_2 \to T_1^\star$	$x_1 \to -x_2$ $x_2 \to -x_1$
v	sheare	$\begin{pmatrix} 1 & 0 \\ -1 & 1 \end{pmatrix}$	1	$T_1 \to T_1$ $T_2 \to e^{i\frac{\Phi}{2}} T_1 T_2$	$x_1 \to x_1$ $x_2 \to x_1 + x_2$
vi	rotation and stretch	$\begin{matrix} -1 & 1 \\ -1 & -1 \end{matrix}$	2	$T_1 \to e^{-i\frac{\Phi}{2}} T_1^\star T_2^\star$ $T_2 \to e^{i\frac{\Phi}{2}} T_1 T_2^\star$	$x_1 \to x_1 + x_2$ $x_2 \to x_1 - x_2$
vii	rotation by $\pi/3$	$\begin{pmatrix} -1 & -1 \\ 1 & 0 \end{pmatrix}$	1	$T_1 \to T_2$ $T_2 \to e^{-i\frac{\Phi}{2}} T_1^\star T_2^\star$	$x_1 \to x_2$ $x_2 \to -x_1 - x_2$
viii	reflection at $x = 0$	$\begin{pmatrix} -1 & 0 \\ 0 & 1 \end{pmatrix}$	-1	$T_1 \to T_1$ $T_2 \to T_2^\star$	$x_1 \to x_1$ $x_2 \to -x_2$
Nr.	Description	(ζ_1, ζ_2)		Automorphism	
ix	reverse sign of T's	$(-1, -1)$		$T_1 \to -T_1$ $T_2 \to -T_2$	
x	reverse sign of T_2	$(1, -1)$		$T_1 \to T_1$ $T_2 \to -T_2$	

Table 1: Useful homomorphisms of the Rotational Algebra

Model	**Hamiltonian**	**classical symbol**
Hofstadter	$H_{\text{Hof}} = T_1 + T_2 + \text{h.c.}$	$2\cos(x_1) + 2\cos(x_2)$
Mathieu	$H_\mu = T_1 + \mu\, T_2 + \text{h.c.}$	$2\cos(x_1) + 2\mu\, \cos(x_2)$
second neighbour	$H_\epsilon = T_1 + T_2 + \epsilon\,(T_1^2 + T_2^2) + \text{h.c.}$	$2\cos(x_1) + 2\cos(x_2) +$ $2\epsilon\,(\cos(2x) + \cos(2x_2))$
Quantum Pendulum	$H_{\epsilon,k} = \epsilon\,(T_1 + T_2) + k e^{-i\frac{\Phi}{2}} T_1 T_2$ $+ \frac{1}{k} e^{i\frac{\Phi}{2}} T_1 T_2^\star + \text{h.c.}$	$\epsilon\,(2\cos(x_1) + 2\cos(x_2)) +$ $2k\cos(x_1 + x_2) + \frac{2}{k}\cos(x_1 - x_2)$
Triangular lattice	$H_\eta = T_1 + T_2 + e^{-i\eta} T_1 T_2 + \text{h.c.}$	$\cos(x_1) + \cos(x_2) + \cos(x_1 + x_2 - \eta + \phi/2)$
Honeycomb lattice	$H_{\text{ hex}} \begin{pmatrix} 0 & T_1 + T_2 + e^{-i\frac{\Phi}{2}} T_1 T_2 \\ T_{-1} + T^{-2} + e^{i\frac{\Phi}{2}} T_2^{-1} T_1^{-1} & 0 \end{pmatrix}$	none

Table 2: Models, Hamiltonians and classical Symbols

Transformation	Description	Symmetry
Nr. i	rotation by $\pi/2$ (Aubry duality)	$\sigma(\mu) = \mu\sigma(1/\mu)$
Nr. x	reverse sign of T_2	$\sigma(\mu) = \sigma(-\mu)$
Nr. ix	reversion of sign infront of T_j	$\sigma(\mu) = -\sigma(\mu)$
Nr. viii	reflection at $x = 0$	$\sigma(\Phi) = \sigma(-\Phi)$
$\Phi \to \Phi + 2\pi$	flux periodicity	$\sigma(\Phi) = \sigma(\Phi + 2\pi n)$
	parameter space	$\Phi \in [0, \pi]$ $\mu \in [0, 1]$

Table 3: Symmetries of the Mathieu model

Transformation	Description	Symmetry
Nr. iii	reflection at $x = p$	$\sigma(\Phi) = \sigma(-\Phi)$
Nr. ix	reversion of sign infront of T_j	$\sigma(\epsilon) = -\sigma(-\epsilon)$
$\Phi \to \Phi + 2\pi$	flux periodicity	$\sigma(\Phi) = \sigma(\Phi + 2\pi n)$
	parameter space	$\Phi \in [0, \pi]$ $\epsilon \in [0, \infty)$

Table 4: Symmetries of the second neighbour model

Transformation	Description	Symmetry
Nr. ii	rotation by π	$\sigma(\eta, \Phi) = \sigma(\eta + \Phi, \Phi)$
Nr. iii	reflection at $x_1 = x_2$	$\sigma(\eta, \Phi) = \sigma(\eta, -\Phi)$
Nr. iv	reflection at $x_1 = -x_2$	$\sigma(\eta, \Phi) = \sigma(-\eta, \Phi)$
Nr. ix	reversion of sign infront of T_j	$\sigma(\eta) = (-1)^n \sigma(\eta + \pi n)$
$\Phi \to \Phi + 2\pi$	flux periodicity	$\sigma(\Phi) = \sigma(\Phi + 2\pi n)$
	parameter space	$\Phi \in [0, 2\pi]$ $\eta \in [0, \pi]$

Table 5: Symmetries of the triangular lattice model

Transformation	Description	Symmetry
Nr. i	rotation by $\pi/2$	$\sigma(k) = \sigma(1/k)$
Nr. iii	reflection at $x_1 = x_2$	$\sigma(\Phi) = \sigma(-\Phi)$
Nr. ix	reversion of sign infront of T_j	$\sigma(\epsilon) = -\sigma(-\epsilon)$
	reversion of energy $H \to -H$	$\sigma(\epsilon, k) = -\sigma(-\epsilon, -k)$
	derived	$\sigma(k) = -\sigma(-k)$
$\Phi \to \Phi + 2\pi$	flux periodicity	$\sigma(\Phi) = (-1)^n \sigma(\Phi + 2\pi n)$
	parameter space	$\Phi \in [0, 2\pi]$ $k \in (0, 1]$ $\epsilon \in [0, \infty)$

Table 6: Symmetries of the doubly-discrete Quantum Pendulum

	critical point	energy	region				
	x,p		A	B	C	D	E
Ia	$2\pi n,\ 2\pi m$	$2(2\epsilon + k + \frac{1}{k})$	a. max.	a. max.	a. max.	a. max.	a. max.
Ib	$2\pi n,\ \pi(2m+1)$ or $\pi(2n+1),\ 2\pi m$	$-2(k + \frac{1}{k})$	a. min.	a. min.	a. min=IV	saddle	saddle
Ic	$\pi(2n+1),\ \pi(2m+1)$	$2(-2\epsilon + k + \frac{1}{k})$	l. max.	saddle	saddle	saddle	a. min.
II	$\pi n\pm \to \arccos((-1)^{n+1}\frac{\epsilon k}{2})$, $\pi n\mp \to \arccos((-1)^{n+1}\frac{\epsilon k}{2})$	$2\left(\left(1 - \frac{\epsilon^2}{2}\right) k - \frac{1}{k}\right)$	saddle	saddle	a. min= IV	a. min.	—
III	$\pi n\pm \to \arccos((-1)^{n+1}\frac{\epsilon}{2k})$, $-\pi n\pm \to \arccos((-1)^{n+1}\frac{\epsilon}{2k})$	$2\left(-k + \left(1 - \frac{\epsilon^2}{2}\right)\frac{1}{k}\right)$	saddle	—	—	—	—
IV	$t\pm \to \arccos\left(-\frac{\epsilon k}{2}\cos(t)\right)$, $-t\pm \to \arccos\left(-\frac{\epsilon k}{2}\cos(t)\right)$	$-2(k + \frac{1}{k})$	—	—	a. min.	—	—

Table 7: Critical points of the classical symbol for the Quantum Pendulum

References

[1] M. Ya. Azbell. Energy Spectrum of a Conduction Electron in a Magnetic Field. *Sov. Phys. JETP*, 19:3:634, 1964.

[2] A. Barelli and C. Kreft. Braid-Structure in a Harper Model as an Example of Phase Space Tunneling. *J. Phys. I France 1*, pages 1229–1249, 1991.

[3] J. Bellissard. Operator Algebras and Application. In D. E. Evans and M. Takesaki, editors, *vol. II.* Cambridge University Press, Cambridge, 1988.

[4] J. Bellissard. Almost Periodicity in Solid State Physics and C*-algeb ras. In B. Fuglede C. Berg, editor, *The Harald Bohr Centenary*, volume 42:3, pages 35–75. Mat.-Fys. Medd. Danske Vid. Selsk., 1989.

[5] J. Bellissard. Gap Labelling Theorems for Schrödinger Operators. In M. Waldschmidt, editor, *From Number Theory to Physics*, pages 538–630. Springer, Berlin, Heidelberg, New York, 1992.

[6] J. Bellissard, Ch. Kreft, and R. Seiler. Analysis of the spectrum of a particle on a triangular lattice with two magnetic fluxes by algebraic and numerical methods. *J. Phys. A: Math. General*, 24:2329–2353, 1991.

[7] A. Bobenko, N. Kutz, and U. Pinkall. The Discrete Quantum Pendulum. *Phys. Lett. A*, 177:399–404, 1993.

[8] S. Borac. The Discrete Fourier Operator and the Factorization of Polynomials Related to the Rational Harper's Equation. *SFB 288 preprint Nr. 126, TU-Berlin*, 1994.

[9] V. Buslaev and A. Fedotov. Complex WKB Method for Harper Equation i. *Algebra and Analysis. The monodromization of Harper equation*, 6, No. 3:59–83, 1994.

[10] V. Buslaev and S. Fedotov. On a Class of Matrices Related to Harper's Equation. *preprint Mittag-Leffler Institute*, (11), 1993.

[11] V. Buslaev and S. Fedotov. *The Functional Structure of the Monodromy Matrix for Harper's Equation*, volume 70. Birkhäuser Verlag, Basel, 1994.

[12] V. Buslaev and S. Fedotov. *Monodromization and Harper Equation.* Ecole Polytechnique, Paris, France, 1994.

[13] V. Buslaev and S. Fedotov. *Bloch Solutions of Difference Equations*, volume 7 No. 4. 1995.

[14] W. G. Chambers. Linear Network Model for Magnetic Breakdown in Two Dimensions. *Phys. Rev.*, A140:135–143, 1965.

[15] K. Chantelau. On the regularization of Schroedinger operators with Coulombic singularities. *Journal of Mathematical Physics*, 34:4421–4427, 1993.

[16] M. Choi, G. A. Elliott, and N. Yui. Gauss Polynomials and the Rotational Algebra. *Invent. math*, 99:225–246, 1990.

[17] F. H. Claro and G. H. Wannier. *Phys. Rev.*, B19:6068, 1979.

[18] A. Connes. Noncommutative Differential Geometry. *Pub. Math. IHES*, 62:257–360, 1986.

[19] H. Eyring. *J. Chem. Phys.*, 3:107, 1935.

[20] L. D. Faddeev. Discrete Heisenberg–Weyl Group and Modular Group. *Letters in Mathematical Physics*, 34:249–254, 1995.

[21] L. D. Faddeev and R. M. Kashaev. Generalized Bethe Ansatz Equations for the Hofstadter Problem. *Commun. Math. Phys.*, 169:181–191, 1995.

[22] L. D. Faddeev and A. Yu Volkov. Quantum Inverse Transform Method with Discrete Space-Time. *Theor. Math. Phys.*, 92:207–214, 1992.

[23] L. D. Faddeev and A. Yu Volkov. Hirota Equation as an Example of an Intergrable Symplectic Map. *Lett. Math. Phys.*, 32:125–135, 1994.

[24] P. G. Harper. Single Band Motion of Conduction Electrons in a Uniform Magnetic Field. *Proc. Phys. Soc. London*, A68:874–892, 1955.

[25] Y. Hatsugai and M. Kohomoto. *Phys. Rev.*, B42:8282, 1990.

[26] B. Helffer, P. Kerdelhue, and J. Sjöstrand. Le papillon de Hofstadter revisite. *Memoires de la S.M.F., no. 43*, 118:3:1–87, 1990.

[27] B. Helffer and J. Sjöstrand. *Current Topics in Partial Differential Equations.* Kinokuniya Company Ltd, Tokyo, 1986.

[28] B. Helffer and J. Sjöstrand. Multiple Wells in the Semiclassical Limit IV. *Ann. Inst. Henri Poincare*, 46:353, 1987.

[29] B. Helffer and J. Sjöstrand. Analyse Semi-classique pour l'equation de Harper avec application a l'equation de Schrödinger avec champ magnetique. *Memoires de la S.M.F. no. 34*, 116:4:1–113, 1988.

[30] B. Helffer and J. Sjöstrand. Semi-Classical Analysis for Harper's Equation III. Cantor Structure of the Spectrum. *Memoire de la S.M.F. no. 39*, 117:4:1–124, 1989.

[31] B. Helffer and J. Sjöstrand. Analyse semi-classique pour l'equation de Harper II. Comportement semi-classique pres d'un rationnel. *Memoire de la S.M.F. no. 40*, 118:1–139, 1990.

[32] D. Hofstadter. Energy Levels and Wave Functions of Bloch Electrons in Rational and Irrational Magnetic Fields. *Phys. Rev. B*, 14:2239–2249, 1976.

[33] P. Wiegmann I. Krichever, O. Lipan and A. Zabrodin. Quantum integrable systems and elliptic solutions of classical nonlinear equations. *Preprint*, 1996.

[34] S. Ya. Jitomirskaja. Almost Everything About the Almost Mathieu Operator II. In D. Iagolnitzer, editor, *XIth International Congress of Mathematical Physics*, pages 373–382. International Press, 1995.

[35] T. Kato. *Perturbation Theory of Linear Operators.* Springer, Berlin Heidelberg New York, 1966.

[36] C. Kreft. Spectral Analysis of Hofstadter-Like Models. *Thesis, TU-Berlin*, 1995.

[37] D. Langbein. *Phys. Rev.*, 180:633, 1969.

[38] Y. Last. Zero Measure Spectrum for the almost Mathieu Operator. *Commun. Math. Phys*, 164:421–432, 1994.

[39] Y. Last. Almost Everything About the Almost Mathieu Operator I. In D. Iagolnitzer, editor, *XIth International Congress of Mathematical Physics*, pages 366–372. International Press, 1995.

[40] Y. Last and M. Wilkinson. A Sum Rule for the Dispersion Relations of the Rational Harpers's Equation. *J. Phys*, A25:6123–6133, 1992.

[41] R. Peierls. Zur Theorie des Diamagnetismus von Leitungselektronen. *Z. Phys.*, 80:763–791, 1933.

[42] H. Pelzer and E. Wigner. *Z. Physik. Chem.*, B15:445, 1932.

[43] R. Rammal. *J. Phys. France*, 46:1345, 1985.

[44] M. Reed and B. Simon. *Mathematical Methods of Quantum Mechanics Vol. IV.* Acad. Press, NY, 1978.

[45] M. A. Shubin. Discrete Magnetic Laplacian. *Commun. Math. Phys.*, 164:259–275, 1994.

[46] D. J. Thouless, M. Kohmoto, M. P. Nightingale, and M. den Nijs. Quantized Hall Conductance in a Two-Dimensional Potential. *Phys. Rev. Lett.*, 49:405–408, 1982.

[47] A. Bobenko V. Babanov and N. Reshetikhin. Quantum discrete sine-Gordon model at roots of unity: Integrable quantum system on the classical background. *Commun.Math.Phys.*, 175:377–400, 1996.

[48] J. v. Neumann and E. Wigner. Über das Verhalten von Eigenwerten bei adrabatischen Prozessen. *Phys. Zeitschrift*, 30:467–470, 1929.

[49] P. B. Wiegmann and A. V. Zabrodin. Quantum Group and Magnetic Translations; Bethe Ansatz for the Asbel-Hofstadter Problem. *Nucl. Phys. B*, 422:495–514, 1994.

[50] M. Wilkinson. Critical Properties of Electron Eigenstates in Incommensurate Systems. *Proc. Royal Soc. Lond.*, A391:305–330, 1984.

[51] M. Wilkinson and E. J. Austin. Phase Space Lattices with Threefold Symmetry. *J. Phys.*, A23:2529–2553, 1990.

[52] J. Zak. Magnetic Translation Group I and II. *Phys. Rev.*, A134:1602–1606 and 1607–1611, 1964.